

STRUCTURE OF ANTIFERROMAGNETS

M. M. FARZTDINOV

Usp. Fiz. Nauk 84, 611-649 (December, 1964)

1. INTRODUCTION

CRYSTALLINE solids having an ordered magnetic structure can be divided into ferromagnets, ferrimagnets, and antiferromagnets. The magnetically ordered state in crystals exists below a certain transition temperature known as the Curie temperature (T_C). In the case of antiferromagnets, this temperature is frequently known as the Néel temperature (T_N). Magnetic materials with an ordered magnetic structure become paramagnetic above the Curie temperature. Such transitions are usually second-order phase transitions and are accompanied by anomalous changes in several physical properties of a crystal (magnetic susceptibility, specific heat, crystal lattice deformation, etc.).

The magnetic structure of magnetically ordered crystals can, as a rule, be represented by a magnetic unit cell, the repetition of which gives the whole magnetic structure. A magnetic unit cell can be identical with a chemical unit cell or may be several times larger than the latter. Recently, however, magnetic substances have been discovered with a so-called helicoidal structure, the properties of which cannot be described by magnetic cells of finite dimensions.

The magnetic structure of the usual ferromagnets can be described by a magnetic cell with one density of the magnetic moment M . Under the action of exchange forces, the elementary magnets in ferromagnetic materials are aligned in parallel and a resultant magnetization M is established in the macroscopic regions (domains), even in the absence of a magnetic field.

A magnetic cell in ferrimagnets and antiferromagnets consists of several superimposed cells, each of which has its own magnetic moment M_i . For example, the spins in the magnetic cell of NiO-type antiferromagnets may be distributed between four magnetic sublattices: all the spins at the vertices of a cube belong to one magnetic sublattice, while the spins located at the centers of three opposite faces belong to three other sublattices. In antiferromagnets of the MnF_2 type, the spins located at the vertices of the tetragonal cell belong to one sublattice, while the spins at the points of intersection of the space diagonals belong to another sublattice.

In ferrimagnets, the total magnetic moment of a magnetic cell is not equal to zero. Sometimes ferrimagnets are called uncompensated antiferromagnets. Although ferrimagnets are similar in their magnetic

structure to antiferromagnets, their magnetic properties are close to those of ferromagnets.

In antiferromagnets, the total magnetic moment of a magnetic unit cell in the absence of a magnetic field is equal to zero, $\sum_i M_i = 0$. In some antiferromagnets,

the magnetic structure may be divided into two sublattices: the magnetic moments of neighboring sublattices are equal and opposite, $M_1 = -M_2$ (for example, MnF_2 , Cr_2O_3 , etc.). It is frequently convenient to replace the two magnetization vectors M_1 and M_2 with two other vectors

$$\mathbf{m} = \frac{1}{2M_0}(\mathbf{M}_1 + \mathbf{M}_2), \quad \mathbf{l} = \frac{1}{2M_0}(\mathbf{M}_1 - \mathbf{M}_2),$$

where $2M_0$ is the value of the magnetization at absolute saturation, \mathbf{m} is the resultant magnetic moment in units of $2M_0$, and \mathbf{l} is the antiferromagnetic vector along which the magnetic moments of the sublattices M_1 and M_2 are aligned. For the usual antiferromagnets, $\mathbf{m} = 0$ in the absence of a magnetic field. The antiparallel orientation of the magnetic moments of the sublattices in antiferromagnets is due to the exchange forces. However, the exchange forces are isotropic in a crystal and by themselves do not fix the position of the magnetic moments of the sublattices with respect to the crystallographic directions. Magnetic forces of relativistic origin are responsible for the appearance of preferred (natural) antiferromagnetic axes (\mathbf{l}) along which the magnetic moments of the sublattices are directed. These magnetic forces may, without greatly distorting the antiferromagnetic ordering, alter slightly the relative orientations or magnitudes of the magnetic moments. As a result of this, an antiferromagnetic crystal may acquire a small spontaneous resultant magnetic moment $\mathbf{m} \sim v^2/c^2$, where v is the velocity of electrons in an atom and c is the velocity of light. This phenomenon is known as weak ferromagnetism (transverse for $\mathbf{m} \perp \mathbf{l}$, longitudinal for $\mathbf{m} \parallel \mathbf{l}$).

Weak ferromagnetism, like some other properties of antiferromagnets, is sensitive to the crystal symmetry. Antiferromagnets exhibiting weak ferromagnetism form a special class of antiferromagnets, typical of which are the rhombohedral antiferromagnets of the $\alpha\text{-Fe}_2\text{O}_3$ or $MnCO_3$ type, the tetragonal antiferromagnet NiF_2 , etc. The presence of a weak spontaneous magnetic moment in antiferromagnets exhibiting weak ferromagnetism makes them similar in some respects to ferromagnets (the nature of the magnetization curve, hysteresis, etc.). However, be-

cause the magnetic moment is small, weak ferromagnets behave in other respects as normal antiferromagnets.

Normal antiferromagnets (those without weak ferromagnetism) form a large group and include, for example, antiferromagnets of the NiO type, etc.

Another large group consists of antiferromagnets having a laminar structure; they are transition metal halides (FeCl_2 , NiCl_2 , MnCl_2 , etc.). These compounds are characterized by structures in which the magnetic ions (Fe^{2+} , Ni^{2+} , etc.) and the halide ions (Cl^-) are located in alternate layers. The ferromagnetic binding in a layer of magnetic ions (the ferromagnetic layer) is much stronger than the antiferromagnetic binding between layers. Because of this, the value of θ in the Curie-Weiss law for these antiferromagnets is positive, i.e., the same as for ferromagnets. In view of these special magnetic properties, such antiferromagnets are sometimes called metamagnets.

Metal antiferromagnets, which we shall not consider here, belong to a special antiferromagnetic group.

Detailed reviews of the work on antiferromagnetism have been published by A. S. Borovik-Romanov^[1] and T. Nagamia et al.^[1]

In the absence of an external magnetic field, ferromagnetic samples divide into macroscopic regions—domains—with different directions of the spontaneous magnetization. Transition layers—domain boundaries—are formed between these regions and the spins are rotated in these layers. In ferromagnetic samples, the excess energy at domain boundaries is compensated by the energy of demagnetizing fields, which disappear because of the formation of domains in a sample. The shape and dimensions of domains as well as the positions of their boundaries in single crystals are governed mainly by the shape and dimensions of samples (i.e., by the demagnetization factor).

In antiferromagnets which do not exhibit weak ferromagnetism there is no resultant magnetization and consequently there are no free magnetic "charges," producing demagnetizing fields, on the sample surface. However, investigations show that in some cases antiferromagnets divide into macroscopic regions (domains). This was first suggested by Néel back in 1948^[2] to explain certain properties of antiferromagnets. Domains in antiferromagnets are elementary regions of a crystal, in which the magnetic structure is periodic, the period being that of a magnetic unit cell. Transition layers or domain boundaries are formed between the domains.

Domain boundaries in antiferromagnets may be of two types: boundaries formed by the rotation of spins in a transition layer and twin domain boundaries due to the twinning of a crystal when magnetic ordering takes place (cf. Sec. 2).

There are several causes of the formation and stability of the domain structure in antiferromagnets.

In antiferromagnets with many equivalent antiferromagnetic axes, in which several different types of elementary region may form, the domain structure may be produced by magnetic ordering. Magnetoelastic forces and magnetic anisotropy forces, which tend to hold the spins along certain crystallographic directions, play an important role in the formation of the domain structure in antiferromagnets. In real antiferromagnetic crystals, the formation of the domain structure is closely related to the presence of various crystal defects (dislocations, grain boundaries, impurities, etc.), internal stresses and inhomogeneities.

In general, the formation of the domain structure in antiferromagnets which do not exhibit weak ferromagnetism is not favored by energy considerations. The domain state of an antiferromagnetic sample corresponds to a relative and not an absolute free-energy minimum. However, such a domain structure is frequently very stable because of its kinetic origin. It can be destroyed only by external agencies (mechanical stresses, magnetic field) or by special heat treatment which prevents the formation of the domain structure during magnetic ordering.

The domain structure in antiferromagnets exhibiting weak ferromagnetism may be formed due to the presence of demagnetizing fields. However, these domain boundaries are more mobile than those in ferromagnets because of the small resultant magnetic moment.

Domain boundary positions in antiferromagnets are not rigidly fixed because of the absence of demagnetizing fields. They may be displaced, by thermal motion, to the extent of several lattice constants from their equilibrium positions. The mobility of domain boundaries causes an increase in the entropy and, consequently, a reduction in the free energy in the transition layer. For some antiferromagnets, the entropy term in the free energy may, over a certain range of temperatures, exceed the energy increase in the transition layer. Then the formation of domain boundaries in an antiferromagnet is favored by thermodynamic considerations.

The fact that there are several causes for the formation of the domain structure and its stability, and that there is a variety of possible domains and domain boundaries, means that in some antiferromagnets the domain structure is very complex.

The domain structure, which is governed by the relative distribution of the domains and domain boundaries, their shapes and dimensions, greatly affects the various properties of antiferromagnets.

The anisotropic magnetostriction of NiO, which decreases when the temperature increases and disappears at the Néel point (K. P. Belov and R. Z. Levitin^[3]), evidences the existence of the domain structure in antiferromagnets. The magnetostriction was investigated in greater detail on single crystals by other workers.^[4,5] The threshold field (discovered by K. P. Belov and R. Z. Levitin), at which consider-

able magnetostriction appears in antiferromagnetic NiO, is evidently associated with the existence of twin domains (cf. Secs. 2 and 3) in polycrystalline samples. The threshold field has not been detected in crystals without twinned domains.^[5] The magnetostriction (10^{-6}) is a quadratic function of the magnetic field up to several kOe, and is anisotropic and reversible.^[5] This type of magnetostriction in NiO is explained mainly by the displacement of the antiferromagnetic domain boundaries in the (111) planes. This conclusion is in satisfactory agreement with the calculations of Alberts and Lee.^[5] Guire and Crapo^[6] investigated the magnetostriction of NiO, MnO, and CoO samples containing twin domains. They explained the magnetostriction of these compounds in terms of the displacement of the twin domain boundaries.

The magnetostriction associated with domain structure was observed also in hematite, α -Fe₂O₃.^[7]

K. P. Belov and R. Z. Levitin^[8-11] observed another interesting phenomenon in the antiferromagnets Cr₂O₃, NiO, CoO, and MnO: anomalies of the elastic modulus and internal friction. Near the Néel temperature, the elastic modulus had a discontinuity and there was an internal friction maximum. Anomalies in these two properties were observed also at lower temperatures.^[11] For example, the internal friction of NiO and CoO had a second maximum below the Néel temperature, and the magnitude of this maximum was sensitive to heat treatment of the sample. Anomalies of the magnetoelastic properties were also discovered in CoO and NiO by other workers.^[12,13] Recently, anomalies of the magnetoelastic properties of hematite α -Fe₂O₃^[14] and some metal antiferromagnets^[15] have been discovered.

The cause of these effects in antiferromagnets, as in ferromagnets, lies in the fact that the application of mechanical stresses to antiferromagnets alters their magnetic (spin) and domain structure. The behavior of the elastic modulus of antiferromagnets near the Néel temperature is explained by two causes, namely, changes in the magnetic (spin) and domain structure, while the anomalous behavior of the elastic modulus at lower temperatures is explained mainly by changes in the domain structure—spin rotation in the domains and displacement of the domain boundaries. Similarly, the second internal friction maximum of NiO and CoO at lower temperatures is explained by the relaxation losses in the domain boundary displacement under the action of mechanical stresses.^[11]

The existence of the domain structure is also used to explain the ΔE effect (change in Young's modulus on the application of a magnetic field) observed in antiferromagnetic NiO, CoO, and MnO.^[9-11] The magnitude of the ΔE effect decreases on approach to the Néel temperature. A ΔE -effect "viscosity" has also been discovered: the value of $\Delta E/E_0$ decreases on prolonged application of a magnetic field. This last effect is also explained by the losses in the processes

of the antiferromagnetic domain boundary displacement under the action of mechanical stresses.

Recently, some success has been achieved in the development of methods for the experimental study of the domain structure of antiferromagnets: the neutron diffraction method and optical methods.^[16-23] Using these two techniques, Roth and Slack^[16-19] investigated the domain structure in an antiferromagnetic single crystal of NiO. They detected experimentally, and investigated, twin domain boundaries and boundaries associated with spin rotation (cf. Sec. 2). Kondoh used an optical method to study the twin domain structure of antiferromagnetic NiO.^[23]

Interesting results on the twin domain structure of NiO were obtained by an x-ray method.^[24]

The neutron diffraction method was used to detect domains in antiferromagnets with laminar structure—cobalt and manganese halides.^[20-21]

Use of the polarized neutron diffraction method makes it possible to detect the presence of 180° domains in antiferromagnets of known structure. Recently, this method has been applied to the study of the domain structure of MnF₂ and α -Fe₂O₃.^[22]

The domain structure of antiferromagnets exhibiting weak ferromagnetism was investigated by the magneto-optic method,^[26-28] the powder figure method,^[28-29] and the electron shadow pattern method.^[30-31]

The nuclear magnetic resonance method has also been used to detect the domain structure in antiferromagnets. Thus, for example, the recent nuclear resonance experiments of Shul'man^[32] indicated the presence of domain boundaries in NiF₂.

The results from the nuclear magnetic resonance method^[33] have indicated the stability of the domain structure in antiferromagnetic α -Fe₂O₃.

The influence of domain boundaries on the antiferromagnetic resonance line in the far infrared was detected for NiO.^[34]

The results of measurements of the magnetoelectric effect in Cr₂O₃, carried out by Rado and Folen, as well as by Astrov^[35], established the existence of domains.

Studies of the magnetic anisotropy, magnetic susceptibility, and magnetization curves of single crystals of NiO, MnO, CoO^[6,36-38], and of rhombohedral crystals of MnCO₃^[39] and CoCO₃^[40] also confirmed the domain structure. Hysteresis effects, indicating the presence of domains, were detected in rhombohedral crystals exhibiting weak ferromagnetism (CoCO₃),^[40] in NiO-type crystals,^[6] in bromides and chlorides of some metals of the iron group,^[41] in some other antiferromagnets,^[42] and in several metal antiferromagnets.^[43]

Apart from the facts which indirectly confirm the domain structure of antiferromagnets, direct experimental observations of the domain structure have been made. This structure has a considerable influence on

such practically important effects as the magnetostriction, magnetoelastic effects, magnetization curves and hysteresis effects, antiferromagnetic and nuclear magnetic resonance, etc. Therefore, further experimental and theoretical studies of the domain structure of antiferromagnets is one of the pressing problems in the physics of magnetic phenomena.

The present paper reviews mainly the results of experimental work on the domain structure of antiferromagnets.

Section 2 deals with the domain structure of antiferromagnets, and various domains and domain boundaries discovered in antiferromagnets; the causes of their formation are discussed.

In Sec. 3, the experimental methods of investigating the domain structure are presented and the results obtained by these methods discussed.

In Sec. 4, the conditions for the existence of the domain structure in antiferromagnets and its stability are briefly dealt with.

2. DOMAIN STRUCTURE OF ANTIFERROMAGNETS

2.1. Antiferromagnetic Domains and Domain Boundaries

When antiferromagnetic ordering occurs, the crystal lattice is deformed by contraction (or expansion) along certain crystallographic directions. For brevity, we shall call these directions the contraction (or expansion) axes. In a single-domain region, the contraction and the antiferromagnetic axes remain fixed throughout that region. However, it should be mentioned that the region in which the contraction (expansion) and the antiferromagnetic axes are fixed is not a single-domain region if in that region the magnetic structure periodicity is disturbed. In other words, in a single-domain region the magnetic structure remains coherent.

Two types of domain boundary are possible in antiferromagnets. One type is due to the magnetic twinning of crystals by the rotation of the contraction (expansion) axis when there is a transition from one region to another without a change of the antiferromagnetic axis (cf. Figs. 6–7). Such domain boundaries represent the boundaries of twins and are known as the twin boundaries or T-walls. An antiferromagnetic single crystal has the T-domain structure if it has only the T-domain boundaries separating the antiferromagnetic domains. The twin domain structure has been discovered in NiO-type crystals.

Boundaries of another type separate regions with the same contraction axis but different directions of the antiferromagnetic vector (1). On going over from one domain to another, the spins are rotated in the transition layer. Therefore, they are called the S-domain boundaries (spin-rotation boundaries) (cf. Fig. 1 and 3). If antiferromagnetic regions are separated by S-boundaries, it is said that the sample has

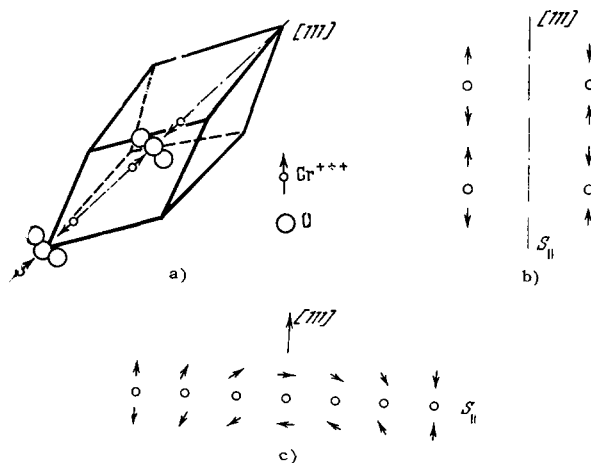


FIG. 1. Domains in Cr_2O_3 . a) Magnetic structure for one of two possible domains in Cr_2O_3 ; b) two antiphase domains separated by an S-type boundary; c) spin rotation schemes for a transition layer S. White circles denote oxygen ions.

the S-domain structure. Antiferromagnetic domains separated by S-boundaries have been detected experimentally by various methods in antiferromagnets of the NiO-type, in $\alpha\text{-Fe}_2\text{O}_3$ and NiF_2 , in Co and Mn halides, and in the uniaxial antiferromagnets Cr_2O_3 , MnF_2 , etc. Antiferromagnets, like ferromagnets, may have 180° , 120° , 90° , etc. domain boundaries, depending on the magnetic and crystallochemical symmetry of the crystal. For example, in accordance with the symmetry, tetragonal NiF_2 crystals may have the 90° and 180° domain boundaries, while rhombohedral $\alpha\text{-Fe}_2\text{O}_3$ -type crystals may have the 60° , 120° and 180° domain boundaries. In the case of the 180° domain boundaries, in uniaxial antiferromagnets, two neighboring domains differ from each other only in the order of the sequence of "plus" and "minus" spins (the sign refers to the vector 1). For example, in chromium oxide, Cr_2O_3 , which is a uniaxial antiferromagnet, the spins of each pair of chromium ions are coupled antiferromagnetically via oxygen ions. The crystal symmetry permits the spin direction along $[111]$ to be either toward or away from the oxygen ions. In accordance with this symmetry, two types of domain, differing only in the order of the sequence of the sublattices in the crystal (Fig. 1b), are possible in Cr_2O_3 . In the case of multiaxial spin structures (NiO , $\alpha\text{-Fe}_2\text{O}_3$), two neighboring domains may differ from each other in the order of the sublattice sequence and in the direction of the antiferromagnetic axes.

In general, some antiferromagnets (NiO and others) may contain both S- and T-boundaries separating different antiferromagnetic domains.

The various possible domains and domain boundaries in antiferromagnets are governed by the magnetic and crystallochemical symmetry of the crystal.

We shall consider below each of these domains and domain boundaries in detail.

2.2. S-domain Boundaries

The forces causing magnetic ordering in crystals are of the exchange type. According to the Heisenberg model, the energy of interaction between two atoms, i and j , is given, to within a constant term, by the expression:

$$E_{ij} = -2JS_iS_j,$$

where S_i and S_j are the vector operators of the spins of the atoms i and j in units of \hbar and J is the exchange integral. The exchange interaction favors the parallel alignment of spins (ferromagnetic ordering) if $J > 0$, and the antiparallel alignment of spins (antiferromagnetic ordering) if $J < 0$.

In many ionic antiferromagnets (NiO , MnF_2 , FeCl_2 , Cr_2O_3 , etc.), the magnetic ions are separated by non-magnetic ions (O^{2-} , F^- , Cl^- , etc.). In this case, the exchange interaction between the magnetic ion spins occurs only via the nonmagnetic ions (the indirect exchange interaction of various types). The theory of the indirect exchange interaction, first developed by Kramers,^[1,44] was extended in the work of Anderson,^[1,44] S. V. Vonsovskii and Yu. M. Seidov.^[44]

In metal antiferromagnets, the exchange interaction between magnetic atoms may occur via the conduction electrons in their collective state.

The problem of the sign of the exchange integral and methods for its calculation have been discussed in the literature for the last 30 years.^[45] The existing methods for the calculation of the exchange integral are still very imperfect. The difficulties of the determination and calculation of the exchange integral have been recently discussed by Overhauser and Herring.^[45]

In antiferromagnets, any departure from the antiparallel alignment of the magnetic ion spins increases the exchange energy.

The magnetic anisotropy forces restrain the sublattice magnetization vectors along certain directions known as natural or preferred magnetic axes. For example, in antiferromagnetic Cr_2O_3 the spins are directed in opposite directions along the $[111]$ axis, i.e., the sole antiferromagnetic axis coincides with the $[111]$ crystal axis. In hematite, $\alpha\text{-Fe}_2\text{O}_3$,^[46] in the temperature range $250^\circ\text{K} < T < 950^\circ\text{K}$, the spins lie in one of the symmetry planes at a small angle ($\approx v^2/c^2$) to a (111) plane, i.e., hematite has three antiferromagnetic axes.

The nature of the magnetic anisotropy energy is governed by the crystallochemical symmetry of the crystal. This energy should be invariant under all transformations permitted by the crystallochemical symmetry and it is an even function of the sublattice magnetization vectors (or the vectors \mathbf{l} and \mathbf{m}).^[47] The value of the anisotropy energy is governed by the so-called second-order, fourth-order, sixth-order, etc. anisotropy constants, which are coefficients of independent homogeneous polynomials of the same order containing components of the vectors \mathbf{l} and \mathbf{m} . The

ratios between the fourth- and second-order, the sixth- and fourth-order anisotropy constants, etc., are of the order of v^2/c^2 . The anisotropy energy is minimal when the antiferromagnetic vector \mathbf{l} is directed along a natural antiferromagnetic axis. Any departure of the spins from the antiferromagnetic axis increases the anisotropy energy.

The transition layers between various domains are formed by the gradual rotation of the sublattice magnetization vectors. The transition layer thickness and the nature of the rotation of the sublattice magnetization vectors are determined by the competition between two forces: the exchange forces tending to make the transition between two domains smoother, and the magnetic anisotropy forces tending to make this transition sharper. The magnetoelastic energy may also play an important role in the formation of domain boundaries because of the magnetostriction. In contrast to ferromagnets, the resultant magnetization of antiferromagnetic crystals free from weak ferromagnetism is very small in the transition layer and usually does not exceed v^2/c^2 in units of $2M_0$. Therefore, the magneto-static energy does not play a decisive role in the formation of domain boundaries in such antiferromagnets.

At 0°K , the law of rotation of the magnetic moments of the sublattices (or the vectors \mathbf{l} and \mathbf{m}) in the transition layer is found from the condition for the minimum of the total transition layer energy, consisting of the exchange energy, anisotropy energy, magnetoelastic energy, and magnetostatic energy.

The main role in the formation of domain boundaries in various antiferromagnets is played by the second-order or higher anisotropy constant, depending on the magnetic structure.

In uniaxial crystals in the antiferromagnetic state, the spins may be, depending on the sign of the second-order anisotropy, either parallel to the principal axis of the crystal (positive second-order anisotropy constant) or located in a plane perpendicular to this axis, i.e., in the basal plane (negative second-order anisotropy constant). In the former case, the rotation of spins in the transition layer takes place in a plane parallel to the principal axis and the second-order anisotropy constant plays the main role in the domain boundary formation. Among such antiferromagnets are Cr_2O_3 , MnF_2 , etc. In the latter case, the domain boundaries are usually formed by the rotation of the spins in the basal planes. In such crystals the anisotropy forces, represented by the second-order anisotropy constant, simply restrict the spins to that plane but do not affect greatly the direction of the spins in the plane itself. The spin orientation in the basal plane is governed by the higher order anisotropies (of the fourth and sixth orders). For example, in NiF_2 , NiO -type crystals, and $\alpha\text{-Fe}_2\text{O}_3$ the domain boundary formation is governed mainly by the fourth- and sixth-order anisotropy constants, which represent the magnetic anisotropy in the basal plane.

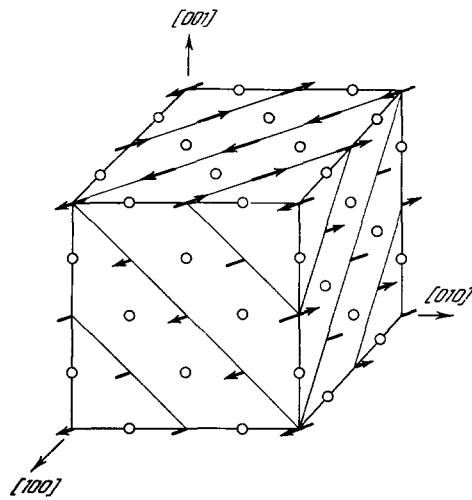


FIG. 2. Antiferromagnetic structure of NiO. White circles are oxygen ions.^[19]

In antiferromagnets free from weak magnetism, whose magnetic structure consists of two sublattices, the S-domain boundaries are formed by the rotation of the vector \mathbf{l} .^[48] In the uniaxial antiferromagnet Cr_2O_3 , the domain boundaries may form along the $[111]$ axis (Figs. 1b and 1c). The resultant magnetic moment in the transition layer is very small and of the order of v^3/c^3 in units of $2M_0$. In other uniaxial antiferromagnets (MnF_2), there is no resultant magnetization in the transition layer ($\mathbf{m} = 0$).

In antiferromagnets exhibiting weak ferromagnetism of the $\alpha\text{-Fe}_2\text{O}_3$ -type, we may have domain boundaries perpendicular to the (111) plane and a symmetry plane, as well as domain boundaries parallel to the (111) plane. The transition layers are formed by the rotation of the antiferromagnetic vector \mathbf{l} and the ferromagnetic vector \mathbf{m} , which may deviate from the (111) plane only by a small angle ($\vartheta \sim v^2/c^2$). The value of the magnetic moment m in the transition layer is constant to within v^2/c^2 and equal to its value in the domains.

In some orthoferrites of the YFeO_3 , LaFeO_3 , and LuFeO_3 type, for which the ferromagnetic vector \mathbf{m} is directed along the c -axis, the domain boundaries are parallel to that axis. The transition layer is formed by the rotation of the antiferromagnetic vector \mathbf{l} ; the vector \mathbf{m} remains parallel to the c -axis but its magnitude decreases on approach to the middle of the transition layer where \mathbf{m} vanishes and its direction reverses.

We shall consider now, in greater detail, the domain boundaries in antiferromagnetic NiO because the data on its domain structure are more complete than those for other antiferromagnets.^[16-19,23,24]

The Néel temperature of nickel oxide NiO is $T_N = 523^\circ\text{K}$, above which NiO is in the paramagnetic state and its crystals are cubic. Below the Néel temperature T_N , the crystal lattice of NiO is deformed, by the antiferromagnetic ordering, into the rhombohedral

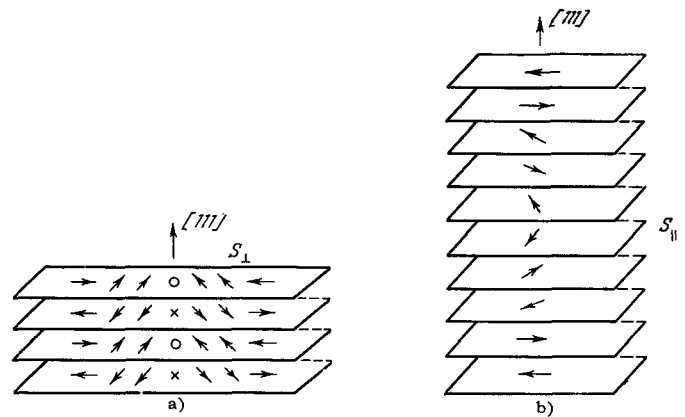


FIG. 3. Two variants of an S-domain boundary in NiO. For simplicity, only the 180° boundaries are shown.

type, by contraction along one of the diagonals $\langle 111 \rangle$ of the original cubic lattice. The distortion of the lattice increases with cooling. To describe the properties of the crystal, it is convenient to use a rhombohedral cell containing 4NiO and having a rhombohedral angle of $90^\circ 4'$ at room temperature. In a unit cell, the Ni^{2+} ions are distributed in four magnetic subcells.

The magnetic structure of NiO below the temperature T_N , determined by neutron diffraction,^[16,18,19] is shown in Fig. 2. The atomic spins lie in planes parallel to the (111) plane. The spins in each plane are parallel (ferromagnetic layers) and antiparallel in neighboring planes.

The direction of the spins in the (111) plane coincides with one of the directions of the $\langle 1\bar{1}0 \rangle$ type, which are antiferromagnetic axes. Such a spin distribution is in agreement with theoretical calculations.^[50,51]

NiO crystals with one contracted $[111]$ axis, i.e., without any T-boundaries, may have a multidomain structure with many S-boundaries. Using the magnetic cell symmetry, Roth^[19] predicted the existence of two types of S-boundary: S_{\parallel} boundaries, parallel to the ferromagnetic layers, and S_{\perp} boundaries, perpendicular to the ferromagnetic layers and containing the rhombohedral axis. In a domain boundary of the S_{\parallel} type, the direction of spins is constant within each ferromagnetic layer, but it does change when there is a transition from one layer to another (Fig. 3b). Conversely, in a boundary layer of the S_{\perp} type, the directions of spins in each ferromagnetic layer vary without disturbing the antiparallel orientation of spins in two neighboring layers (Fig. 3a). Since the anisotropy in the (111) plane is small ($3 \times 10^3 \text{ erg/cm}^3$ ^[6]), various S-boundaries are possible in NiO but the most stable may be the boundaries between regions whose spin directions make angles $\pi/3$, $2\pi/3$, or π . By virtue of the symmetry of the NiO magnetic cell, these angles correspond to the angles between the three natural antiferromagnetic axes in the (111) plane. S-boundaries in antiferromagnets of the NiO type, have been studied theoretically in^[48].

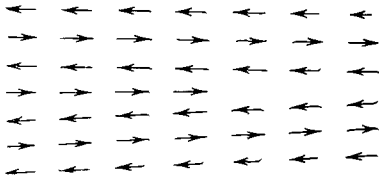


FIG. 4. Formation of an S-boundary at a dislocation. Traces of (111) planes on a (100) plane are shown.

The presence of two types of S-boundary in NiO is explained by the nature of the interaction between the spins; their formation is related to the presence of several equivalent antiferromagnetic axes and the relatively weak anisotropy in the (111) plane. The spins in a ferromagnetic layer have an exchange interaction along $\langle 110 \rangle$, while the spins in neighboring layers are paired antiparallel due to a strong indirect exchange interaction through the oxygen ions along $\langle 100 \rangle$.

It follows from the nature of the distribution of magnetic moments in the transition layers of the S_{\parallel} and S_{\perp} boundaries in NiO that the S_{\parallel} boundaries may have a small magnetic moment, while the S_{\perp} boundaries should have no magnetic moment. Hence, it follows that the two types of boundary may be distinguished experimentally by their behavior in a magnetic field. This difference has not yet been detected experimentally. However, studies of the magnetic field dependence of the susceptibility along [111] in NiO have shown^[6] that the susceptibility curve obtained by increasing the field up to 25 kOe lies somewhat lower than the curve obtained when the field is decreased. This weak susceptibility hysteresis may be due to the weak magnetic moment of the domain boundaries.^[2]

In real antiferromagnets, more complex S-boundaries may form, exhibiting a simultaneous departure from the parallelism of spins in a ferromagnetic layer and from the antiparallelism of two neighboring ferromagnetic layers. However, in normal antiferromagnets, in which an indirect exchange interaction of the magnetic ion spins via the nonmagnetic ions is dominant, the preferred boundaries are of the S-type associated with a gradual rotation of the sublattice magnetization vectors without a marked disturbance of their parallelism. For example, for the laminar structure of NiO, the indirect exchange interaction between the neighboring layer spins is stronger than the exchange interaction within the ferromagnetic layers and therefore the formation of the S_{\perp} boundaries in NiO should be energetically preferred to the S_{\parallel} boundary formation.

Conversely, in compounds where the interaction between the magnetic ions in a ferromagnetic layer is stronger than the antiferromagnetic coupling between the magnetic ions in two neighboring layers, the preferred formation of the boundaries is associated with a gradual departure from the antiparallelism in two neighboring layers. Among such compounds, are anti-

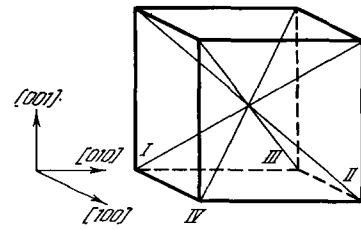


FIG. 5. Orientation of T-regions in NiO. The rhombohedral axes are taken relative to the initial cubic lattice.^[19]

ferromagnets (metamagnets) having a laminar structure—halides of metals in the iron group.

The problem of the formation and stability of boundaries in pure antiferromagnets will be discussed in Sec. 4. In real antiferromagnets, the boundary positions may be governed by crystal and magnetic defects (twins, grain boundaries, dislocations, etc.). Figure 4 shows the formation of S-boundaries at an edge dislocation. The formation of domains when twinning occurs is discussed (Sec. 2.3) and in Sec. 3.2.

2.3. Twin Domain Boundaries

A twin boundary in NiO is a twinning plane and its formation is associated with the twinning of a crystal due to magnetic ordering. On cooling below the Néel temperature T_N , the rhombohedral (contraction) axis may be parallel to any of the four space diagonals of a cube [111], $[\bar{1}\bar{1}1]$, $[1\bar{1}\bar{1}]$, and $[\bar{1}1\bar{1}]$, of the original cubic lattice (Fig. 5). We shall denote these directions by I, II, III, IV, respectively.

From the twinning condition of the NiO crystal, it follows that a domain boundary (a T-boundary) has the lowest energy if the direction of the antiferromagnetic axis in two neighboring domains does not change when there is a transition through a T-boundary and if the ferromagnetic layers intersect on a straight line parallel to the antiferromagnetic axis direction for two neighboring domains. Thus, at some point in the vicinity of the T-boundary, the antiferromagnetic axis is identical for two neighboring domains but the directions of the ferromagnetic layers are different.

Using these conditions, Roth^[19] predicted possible twin domain boundaries in NiO crystals.

Each pair of regions with a common antiferromagnetic axis but different contraction axes, may be joined in two ways: either by one of the $\{100\}$ planes, or by one of the $\{110\}$ planes. Thus, twelve types of T-boundary with six different antiferromagnetic axes (Table I) are possible in NiO. Figure 6 illustrates the domain boundaries of the I(001)II and I(110)II type. In both cases, the antiferromagnetic axes are identical and the ferromagnetic layers are rotated from (111) to $(\bar{1}\bar{1}1)$, but the twinning planes are different: (001) and (110). In the initial magnetic crystal, the T-boundaries (001) and (110) are not reflection planes but glide planes. After twinning, the spins are distributed symmetrically

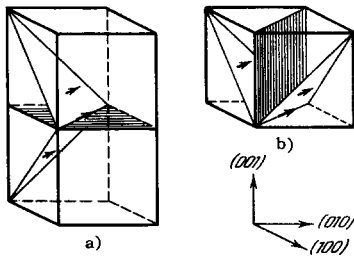


FIG. 6. T-boundaries of the (001)II and I(110)II types (shown hatched). For each domain, the direction of the ferromagnetic layers is shown. The antiferromagnetic axes coincide.^[19]

with respect to the twinning plane, but the T-boundaries are not reflection planes since reflections in such a plane would reverse the directions of the spin component parallel to the reflection plane. Hence, it follows that if twinning is induced by an external stress in a region with one rhombohedral axis, then this partly rotates the spins in even or odd ferromagnetic layers in the vicinity of the T-boundaries. In other words, S-domain boundaries may be produced by twinning (Fig. 7).

It is easy to understand that the formation of T-boundaries is also associated with a departure from the antiparallelism of spins along a twin boundary (cf. Fig. 7). Before twinning, two layers of nickel ions on opposite sides of a twinning plane are coupled by antiparallel pairing via the oxygen ions (Fig. 7a). After twinning, the spins of these ions become parallel (Fig. 7b) although they are coupled, as before, via the oxygen ions. The T-boundary formation may therefore increase the exchange energy and the anisotropy energy. Hence, it follows that the T-boundaries in antiferromagnets cannot be sharp but must have a definite thickness extending over several atomic planes. The finite thickness of the T-boundaries in NiO is con-

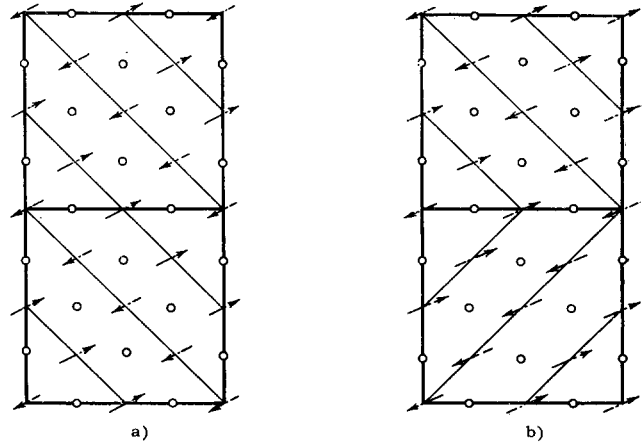


FIG. 7. Cross section of a crystal along (100) before and after twinning. The change in the direction of spins is shown in the lower part of b).

firmed by the experimental data. The visible thickness of the T-boundaries in annealed crystals is of the order of 1μ ,^[23] while the thickness of the domains themselves is of the order of 1 mm.^[19]

3. EXPERIMENTAL STUDIES OF THE DOMAIN STRUCTURE OF ANTIFERROMAGNETS

3.1. Neutron Diffraction Method

a) General remarks. The existence of T and S domain boundaries in NiO has been confirmed by Roth's neutron diffraction studies.^[18,19] The neutron diffraction method is based on the fact that the scattering of neutrons by the $\{111\}$ planes in a magnetic lattice depends on the crystallographic orientation of the ferromagnetic layers but is independent of the direction of magnetization of a given layer. The determination of the magnetic field at various positions in the $\{111\}$ reciprocal lattice gives directly the relative distribution of the I, II, III, IV type regions in a NiO crystal irrespective of whether the S-domain boundaries are present in it. On the other hand, the scattering of neutrons by planes not parallel to (111) is different, depending on the direction of magnetization in a ferromagnetic layer, and may be used to determine T- and S-type boundaries,

b) Studies of the distribution of twin domains. The distribution of the T-domains in NiO crystals grown by various methods has been investigated by scattering neutrons from $\{111\}$ planes. Crystals grown by the Verneuil method or by vapor condensation, as well as natural crystals, have been used.

Experiments have revealed^[19] large variations in the distribution of the magnetic field in the $\{111\}$ planes of crystals cleaved from different ingots. T-regions in such crystals were almost randomly distributed between four possible types. The T-domain structure has been also investigated in annealed crystals.

Table I. T-domain boundaries between the twin domains in NiO^[19]

Domain orientation	I—IV (111)—(1 $\bar{1}\bar{1}$)	I—III (111)—(1 $\bar{1}\bar{1}$)	I—II (111)—(1 $\bar{1}\bar{1}$)
Antiferromagnetic axes	[01 $\bar{1}$]	[1 $\bar{0}$ 1]	[1 $\bar{1}$ 0]
Domain boundaries	(100) (011)	(010) (101)	(001) (110)
Domain orientation	II—III (1 $\bar{1}\bar{1}$)—(111)	II—IV (1 $\bar{1}\bar{1}$)—(111)	II—IV (1 $\bar{1}\bar{1}$)—(111)
Antiferromagnetic axes	[01 $\bar{1}$]	[101]	[1 $\bar{1}$ 0]
Domain boundaries	(100) (011)	(010) (101)	(001) (110)

These crystals were annealed at $T \geq 1500^\circ\text{C}$ in an argon atmosphere containing traces of oxygen (10^{-4}). The annealing altered basically the T-domain distribution in the crystals, making these domains larger. Only two (out of four) types of region were found in the annealed crystals. In cleaved and annealed crystals, approximately one-third of the regions were of type I and two-thirds of type II, while in an annealed thin plate two-thirds were of type III and one-third of type IV, the ratio being opposite in another plate. A similar result was obtained for crystals prepared by vapor condensation on the (100) plane: about one-fifth of the regions were of type II and four-fifths of type III.

This was because, as will be shown, the samples consisting of two regions were the most stable (cf. Sec. 3).

Slack^[17] proposed a method for preparing NiO crystals without T-boundaries by annealing at $T > 1500^\circ\text{C}$ in argon without applying external stresses. After cooling to 25°C , a short application of an external stress ($\approx 10^6 \text{ dyn/cm}^2$) along [111] removed almost all the T-domain boundaries. Thus, one could obtain a crystal having 98.7% of type I regions, i.e., a crystal almost free of twin boundaries.

c) Studies of S-domain boundaries. The neutron diffraction method is, so far, the only method available for the direct observation of the S-domain structure in antiferromagnets free from weak ferromagnetism.

The neutron diffraction method has yielded some data on the distribution of spins in the (111) plane of NiO crystals free of T-boundaries.^[19] The results of the neutron-diffraction measurements on a pure crystal have indicated the presence of S-boundaries and a uniform distribution of spins among domains with the $\langle 110 \rangle$ spin directions, i.e., the S-domain boundary distribution has been found to be random. Hence, it follows that the susceptibility in the (111) plane should be isotropic, in accordance with the experimental results on the torque in weak fields.^[36] However, because of a large correction for the secondary extinction, it has not been possible to carry out an accurate analysis of the S-boundary distribution in a pure crystal.

The neutron diffraction method has been used also to study the rotation of spins and the motion of boundaries in NiO under the action of a magnetic field ($H \perp [111]$). Owing to the difference between the transverse and longitudinal susceptibilities ($\chi_{\perp} > \chi_{\parallel}$), the spins in the (111) plane have tended to align themselves perpendicular to the magnetic field direction H . The spin rotation or the displacement of S-boundaries in the (111) plane has occurred in fields $H \geq 2400 \text{ Oe}$. The spin distribution in the absence of a magnetic field has been found to depend on the prior magnetic history of the sample. Some hysteresis has been found in the rotation of the spins in the (111) plane. According to torque measurements, the energy dissipation in an untwinned NiO crystal, associated with the spin rotation in the (111) plane in a magnetic field, reaches a maxi-

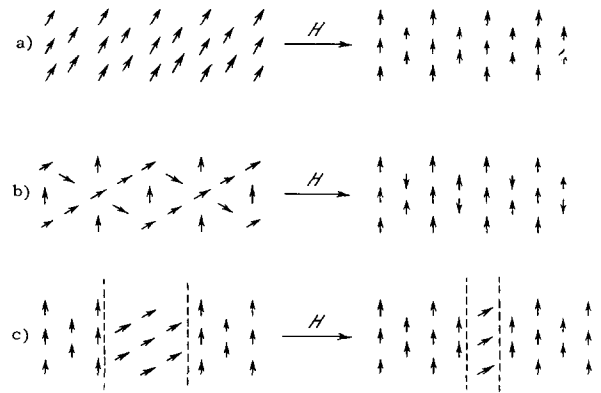


FIG. 8. Rotation of spins in a domain in NiO, situated in a magnetic field.^[19]

imum value of 375 erg/cm^3 per period at 8000 Oe and decreases slightly with further increase in the field.^[16]

The spin rotation in weak and moderate fields has not been detected in planes other than (111), owing to the strong anisotropy of NiO outside this plane.

The rotation of magnetization in the (111) plane may take place either by the coherent rotation of the spins in the domains or by the displacement of the domain boundaries. The coherent rotation of the spins in the domains varies with the nature of the interaction between the spins in the (111) plane. Figures 8a and 8b show the coherent rotation of the spins in a domain for strongly and weakly paired spins of various sublattices in the (111) plane. Figure 8c shows the displacement of the boundaries by an increase in the dimensions of those domains in which the spins have components parallel to the magnetic field direction.

Investigations of the magnetic anisotropy^[16] have shown that in moderate fields of $2400 < H < 8000 \text{ Oe}$ the spins rotate or the domain boundaries are shifted (Fig. 8c), while in $H > 8000 \text{ Oe}$ there is a coherent rotation of the spins in the (111) plane. These data agree approximately with the results obtained by investigating the spin rotation in a magnetic field by the neutron diffraction method. The test results on neutron diffraction show that about 49% of the spins are rotated at 4800 Oe and about 60% at 6000 Oe.

The neutron-diffraction method has also indicated a domain structure in cobalt and manganese halides (CoCl_2 , CoBr_2 , MnCl_2 , etc.).^[20,21] In these laminar structures, the spins lie in parallel planes containing the three antiferromagnetic axes, which meet at 60° with one another. In CoCl_2 and CoBr_2 , the spins in each layer are parallel (ferromagnetic coupling) and antiparallel in neighboring layers. In cobalt halides, one may have various combinations of S-boundaries of the type considered, while in manganese halides the domain structure is more complicated.

In the absence of a magnetic field, the domains in these compounds are approximately uniformly distributed between the three equivalent antiferromag-

netic axes. In a magnetic field weaker than 10 kOe, the domain boundaries are displaced so as to increase the volume of the domains with the antiferromagnetic axis perpendicular to the magnetic field. In moderate fields (less than 10 kOe), the domain boundaries are shifted irreversibly. By applying a magnetic field in the plane of a layer at right angles to the antiferromagnetic axis of one of the domains, one may produce a region which consists almost entirely of a single domain.

In the investigated antiferromagnets (NiO, transition-metal halides, etc.) the displacement of the S-boundaries in a magnetic field occurs approximately between 2000 and 10 000 Oe, in agreement with Néel's estimate.^[2]

The presence of domains with 180° boundaries can be detected in antiferromagnets by means of polarized neutrons.^[22]

The dependence of the neutron scattering on the polarization may be described by means of the ratio of the intensities of scattered neutrons of opposite polarizations

$$R = \frac{I_+}{I_-} = \frac{(N+M)^2}{(N-M)^2},$$

where N and M are, respectively, the nuclear and magnetic structure factors. The magnetic structure of an antiferromagnet is sensitive to the polarization ($R \neq 1$) if the sites in different magnetic sublattices with oppositely directed spins are related by one of the symmetry elements of the space group, except translation, and the magnetic lattice has no antisymmetry center. These requirements are satisfied, for example, by antiferromagnets (MnF_2 and $\alpha\text{-Fe}_2\text{O}_3$), in which the domains have been investigated by means of polarized neutrons.^[22]

In hematite, $\alpha\text{-Fe}_2\text{O}_3$, two types of antiferromagnetic domain have been detected at room temperature when the spins are distributed in the (111) plane. The spins in the domains lie along the three antiferromagnetic axes for each of which there are 180° domains. In the absence of an external magnetic field, the domain distribution is isotropic.

3.2. Optical Observations of a Twinned Domain Structure

a) Observation in transmitted polarized light passing through thin plates.^[19] T-domains in NiO can be seen clearly in transmitted polarized light, using thin plates (100μ or less). Each domain is a uniaxial crystal whose optical axis coincides with the contraction axis. At a T-boundary separating two neighboring domains, the optical axis of the crystal changes its direction so that the two neighboring regions have different optical axes. NiO crystals exhibit birefringence ($n_e > n_o$) and are slightly dichroic. Thin plates appear pale yellow to green in color in transmitted unpolarized light. In polarized light, the color is intensified. To observe the

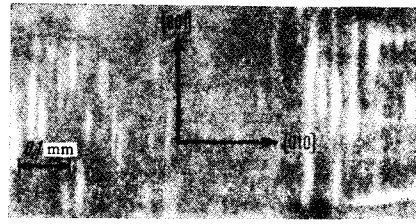


FIG. 9. Polished unannealed thin plate of NiO. Narrow T-regions are shown.^[19]

domain structure in a thin NiO plate, a gypsum $\lambda/2$ plate has been used in the 45° position. Depending on the orientation of the optical axis with respect to the gypsum plate, the color of the domains in the NiO plate varies from light yellow to green.

Microscope observations show the crystallographic orientation of T-boundaries, the growth of domains as a result of annealing, and the displacement of T-boundaries under external mechanical stresses or a magnetic field (cf. Figs. 9–17).

To observe the domain structure, thin plates are prepared by cleaving crystals along the (100) plane. Then the plates are subjected to special polishing to reduce their thickness to 25μ . The plates prepared in this way are examined along the [100] direction. When the projections of the optical axes on the (100) plane coincide for two neighboring domains, the NiO plate has to be inclined at 45° to the microscope axis.

During the polishing process, the surface of a plate becomes deformed and this produces a large number of T-boundaries. In such a plate, the domains are very small, having dimensions of only several microns (Fig. 9). Larger domains may be obtained by annealing the crystal at a high temperature $T \geq 1500^\circ\text{C}$ followed by gradual cooling to room temperature in about an hour. Such domains have dimensions of several milli-

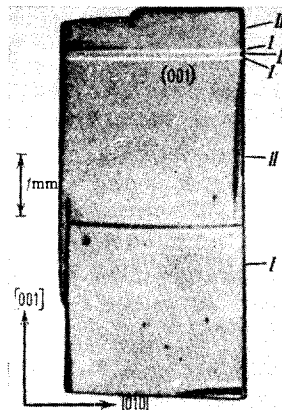


FIG. 10. Annealed NiO crystal with boundaries of the I(001)II type.^[19]

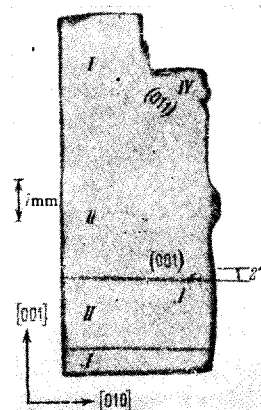


FIG. 11. NiO crystal containing I(011)II and I(011)IV boundaries.^[19]

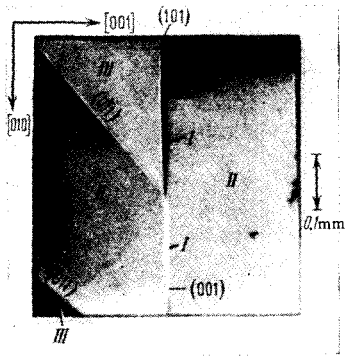


FIG. 12. NiO sample containing four types of T-boundary. Formation of an S-boundary in region III is possible.^[19]

meters and usually extend across the thickness of a plate (Figs. 10–11).

Increase of the domain dimensions with annealing is due to the fact that in unannealed crystals the T-boundary positions are restricted by the presence of some crystal defects such as grain boundaries or impurities; high-temperature annealing removes such defects by diffusion. The T-boundary positions in annealed crystals are determined by the condition of minimum surface energy of the domain boundaries and the shape of the crystal surface.

Well-annealed crystals usually consist of simple combinations of T-boundaries parallel to one of the faces of the crystal lattice. In thin plates, the domain boundaries are usually parallel to the short dimensions of the plate. Obviously, such a distribution of the domain boundaries corresponds to the minimum energy of these boundaries. In some cases, small departures of the T-boundaries from simple crystallographic directions are observed (Fig. 11; see also ^[24]). Evidently this effect results from internal stresses, which are produced by cooling the crystal from 1500°C to room temperature.

In well-annealed crystals, a stable domain structure

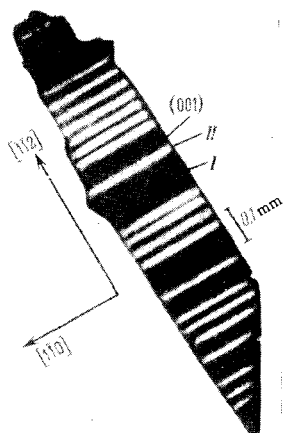


FIG. 13. Simple boundaries of the I(001)II type are shown along the (111) cross section.^[19]

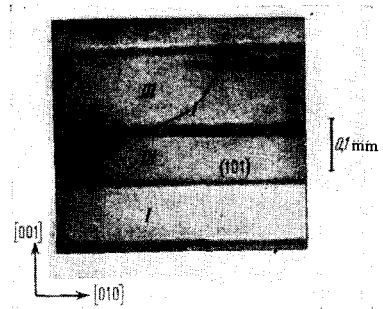


FIG. 14. Laminar regions in a (100) plane.^[19]

is usually formed (cf. Figs. 10 and 13) from regions of two types, obeying the twinning rule given in Table I. However, the presence of two or several regions not related by the twinning rule may rotate the antiferromagnetic axes and thus give rise to S-boundaries. For example, in the sample shown in Fig. 11, the antiferromagnetic axis $[1\bar{1}0]$, associated with the presence of boundaries of the I(001)II type, is dominant but the presence of domain boundaries of the I(011)IV type with the $[01\bar{1}]$ antiferromagnetic axis gives rise to S-domains.

In the sample shown in Fig. 12, there are T-boundaries of the II(011)III, I(001)II, I(101)III types with non-coincident spin axes $[0\bar{1}1]$, $[1\bar{1}0]$, and $[\bar{1}01]$, respectively. Hence, the presence of T-boundaries in such a poorly twinned sample suggests the presence of S-boundaries, the formation of which may be associated both with a change in the direction of a ferromagnetic layer and with a rotation of the antiferromagnetic axes.

Investigations ^[19,23] have shown that the crystal lattice of NiO in the antiferromagnetic state experiences, apart from the contraction along the $[111]$ axis, an additional weak contraction (10^{-6}) along the antiferromagnetic axis $[110]$. Therefore, in the region with a single rhombohedral axis, the various domains surrounded by S-boundaries have slightly different optical

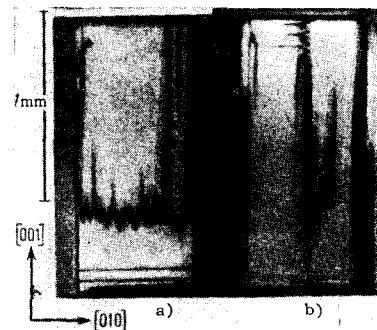


FIG. 15. Displacement and rotation of T-boundaries under the action of mechanical stresses applied along $[001]$. Some of the (101) boundaries moved along $[001]$, while others were transformed into boundaries of the (010) type. It is possible that the latter process occurred in regions of the I–III type, for which the transformation (101)–(010) does not involve rotation of the antiferromagnetic axis (cf., Table I).^[19]

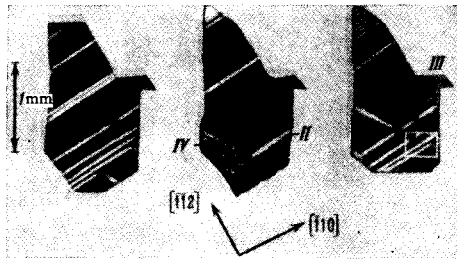


FIG. 16. Displacement of T-boundaries under the action of a magnetic field. Crystal surface (111). A field of 25 kOe, applied first along [112] and then along [110]. The rectangular region is shown on a larger scale in Fig. 17.^[19]

properties. Utilizing this property, Kondoh^[23] employed a highly sensitive polarization microscope to detect in NiO the presence of S-domains in the form of narrow parallel bands. The domain dimensions were 0.1–0.01 mm.

b) Specular reflection method. Samples thicker than 0.5 mm transmit too little visible light for the observation of T-boundaries. An attempt to observe the T-domain structure by coating the crystal surface with a suspension of Fe₂O₃ has also failed to give a positive result. But it has been found possible to observe the T-domain structure in larger NiO crystals by the specular reflection method.^[17]

In view of the slight distortion of the cubic NiO lattice below the Néel point, the faces of two neighboring regions in a twinned crystal may make a small angle of between 2.5' and 12'. Figure 18 shows two twinned regions whose lateral surfaces form a small angle η . If such faces of two twin regions emerge on the crystal surface, they may be observed by the specular reflection method. For this purpose, the crystal surface is polished to optical flatness in order to observe the specular reflection of light. For a crystal in the form of a rectangular parallelepiped, all six faces may be polished (cf. Fig. 20). Many domain boundaries appear on the surface and in the interior of the crystal as a result of polishing. If such a polished crystal is an-

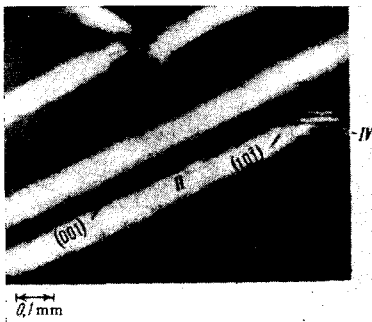


FIG. 17. Details of the rectangular region shown in Fig. 16. A stressed region is visible where a type II region has moved, together with a smooth transition between II and IV type regions, having boundaries of the (101) type.^[19]

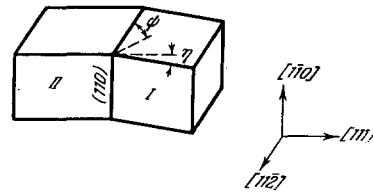


FIG. 18. Angle of tilt η , formed at a I(110)II boundary shown on an enlarged scale for the front face of a crystal. At the top face, $\eta = 0$. The angle of tilt Ψ between a T-boundary and a (111) plane is also shown.^[16]

nealed at a high temperature, the majority of the small T-domains disappears and only a few larger T-domains remain. Slight roughness appears in the untwinned part of such a crystal due to the disappearance of the T-boundaries present before annealing. This roughness brings out the specular reflection of the corresponding crystal face. Some of the T-boundaries which remain after annealing may be observed if the angle between the faces of two twinned regions is not equal to zero on the polished surface. Detailed observations of the light reflected from a polished and annealed crystal have shown that all the T-boundaries which end at the surface may be observed. The majority of them can be seen with the naked eye and smaller ones can be seen under a microscope. If a T-boundary does not give rise to a non-zero angle between the faces of two neighboring regions on a given crystal surface, the presence of a T-boundary and its position may be determined from its appearance at other crystal surfaces (Figs. 19 and 20). The values of the tilt angles for various T-boundaries on various crystal faces of NiO are given in ^[17,24].

If a crystal has several twinned regions, then the T-boundaries separating them should end at the crystal surface. This can be easily shown by comparing complex twinned regions consisting of two, three, etc. regions of various types. If a twin boundary does not emerge at the surface, it means that the crystal is incompletely twinned.

The observations of the specular reflection method show that a crystal may have many T-boundaries in various combinations. For example, Fig. 19a shows a

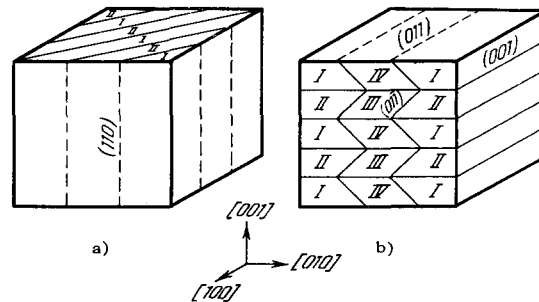


FIG. 19. Possible multi-twin structures in unstressed crystals.^[16]

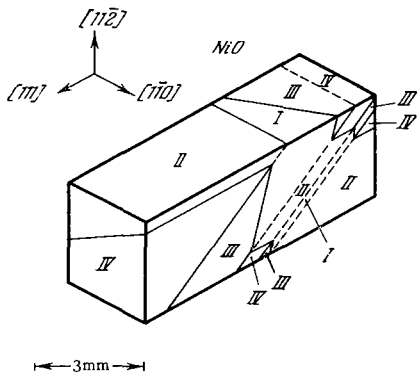


FIG. 20. Twin boundaries observed by the specular reflection method on surfaces of an annealed crystal. Visible T-boundaries are shown by continuous lines, invisible ones by dashed lines.^[16]

crystal with a laminar structure consisting of alternating type I and II regions, twinned by planes of the (110) type. The continuous lines show T-boundaries with non-zero tilt angles between neighboring faces, while the dashed lines show T-boundaries with zero tilt angles. This multi-twin crystal, which was found among well-annealed crystals, was almost free of internal stresses. Preliminary calculations showed that the free energy per unit area of the domain boundary was quite small and the T-boundary positions shown in Fig. 19b could be fixed by small crystal defects.

More complex multidomain structures with very low energy per unit volume may exist in a crystal if the T-boundaries intersect. It follows from Table I that it is possible to form structures with several (2, 3, 4, 5, etc.) T-boundaries intersecting along a common line. The lowest energy per unit volume is obtained for regions formed by the intersection of four boundaries (Fig. 19b). Samples of this type (cf. Fig. 19b) have, in fact, been observed among well-annealed crystals (Fig. 20; see also^[23,24]).

The elastic energy per unit volume of such crystals is very small and amounts only to 10^{-2} erg/cm³. In samples with other combinations of T-boundaries, the elastic energy per unit volume is much higher and reaches 10^5 erg/cm³. The same applies to unannealed crystals. Using the specular reflection method, we may detect domains having dimensions of 1 mm or larger in well-annealed crystals; if the twin domain dimensions are 0.1 mm or less, the specular reflection method cannot be used to detect the presence of T-domains in a crystal.

c) Some results obtained by optical methods. T-boundaries in well-annealed NiO crystals are highly mobile and may move through a crystal on the application of a mechanical stress or a magnetic field. During heat treatment, T-boundaries may move by distances of several millimeters and their motion may be observed in polarized light using an optical microscope.

The motion of T-domain boundaries under the ac-

tion of mechanical stresses is due to the fact that the elastic energy is lowest for those domains for which the contraction axis is parallel to the applied stress. Therefore, the action of mechanical stresses enlarges the domains whose contraction axes are parallel to the applied stress.

If moderate stresses are applied for a fraction of a second, the T-boundary displacement is elastic; in the unstressed state, the boundaries return to their initial positions. However, if the T-boundaries remain in the displaced position for 10–20 sec, their motion becomes irreversible. If we repeat the T-boundary displacement many times, the motion becomes viscous and the boundaries become fixed: “mechanical hardening” occurs. The mobility of the domain boundaries is recovered if the deformation is not too great and the crystal is rested for several days at room temperature.

Domains may be altered from one type to another by applying external mechanical stresses. After its removal from the annealing furnace, a crystal may have a simple domain structure consisting of several boundaries of the (011) type (cf. Fig. 15a). By applying external stresses almost normally to domain boundaries, these boundaries are made zig-zag in shape with the main component parallel to the external stress direction (cf. Fig. 15a). Obviously, such complex boundaries are formed by the intersection of various laminar T-boundaries. Laminar T-regions with complex boundaries may move easily across the whole crystal. For one of the types of motion, the angle between the T-boundaries remains constant and the complex zig-zag boundary moves parallel to itself. For other types of motion, the angle between T-boundaries changes and wedges penetrate a neighboring region in the form of thin spikes.

Microscope observations were made of the dependence of the T-domain structure on the distribution of local internal stresses during heat treatment. On heating, the crystal became isotropic and above the Néel temperature (T_N) the domains disappeared altogether. If the crystal was cooled after heating above the Néel temperature, the domains reappeared. After the heat treatment, the T-boundary distribution in a crystal was different from that before the treatment. With repeated heat treatment, the domain boundaries reappeared during cooling stage, usually at the same positions, i.e., the T-boundary distribution altered only after the first heat treatment cycle. The sensitivity of the T-boundaries to temperature was re-established on the application of very small stresses which redistributed inhomogeneities in the crystal. These observations show that in real crystals the T-domain structure depends strongly on external stresses and on inhomogeneities.

In well-annealed NiO crystals, the motion of twin domain boundaries in a magnetic field begins in fields of 5000 Oe, while stronger fields rotate the spins; in such crystals the T-boundaries move or rotate to new

positions in fields up to 20–30 kOe.

In untwinned NiO single crystals, the displacement of the S-boundaries or the rotation of the spins in the domains occurs in the (111) planes, which have weak anisotropy (3×10^3 erg/cm³), under the action of a magnetic field component parallel to the (111) plane. In poorly twinned crystals, the planes of the (111) type are distributed at random with respect to an external magnetic field. Therefore, in polycrystalline and twinned samples, the magnetostriction is mainly due to the displacement of the T-boundaries in a magnetic field, as indicated by the magnetostriction threshold field of 5000 Oe. No threshold magnetostriction field has been found in untwinned single crystals of NiO. The magnetostriction in such crystals is reversible and increases quadratically with the field up to several kOe. Such magnetostriction is due to the displacement of the S-boundaries of domains in which the spins lie in the (111) planes.

The influence of a magnetic field on the T-boundaries is basically similar to the influence of external stresses. The sensitivity of the T-boundary position to a magnetic field is very unstable. The new T-boundary positions are evidently associated with local inhomogeneities in real crystals. If a magnetic field is applied several times to a crystal, the T-boundaries frequently become immobilized. If the crystal is then left in the free state for several hours, the sensitivity of the T-boundaries to magnetic fields is re-established. Changes in a T-boundary under the action of a magnetic field are shown in Fig. 16. A crystal which was polished parallel to the (111) plane consisted, after annealing, mostly of regions of the type I with several regions of the type II separated by (001) planes; most of these regions were destroyed by applying a magnetic field of 25 kOe along the [112] direction. Some T-boundaries of the (001) type were displaced in such a way as to increase the volumes of the type II regions while in another part of the crystal new type IV regions and new (100) T-boundaries were formed. When the field was applied along [110], many of the (001) boundaries were re-established.

3.3. Investigation of Domains by Measuring the Torque of a Crystal in a Magnetic Field

The method of measuring the torque of a crystal suspended in a uniform magnetic field may be applied also to the study of the T-domain structure of antiferromagnets.^[17] When applied to a single crystal of NiO, the method is based on the fact that below the Néel temperature T_N the susceptibility $\chi_{\perp 1}$, perpendicular to a ferromagnetic layer, is higher than the average susceptibility in a (111) plane, i.e., $\chi_{\perp 1} > \frac{1}{2}(\chi_{\parallel} + \chi_{\perp 2})$, where χ_{\parallel} is the susceptibility measured parallel to the antiferromagnetic axis in the (111) plane; $\chi_{\perp 2}$ is the susceptibility measured perpendicular to the antiferromagnetic axis in the same plane.

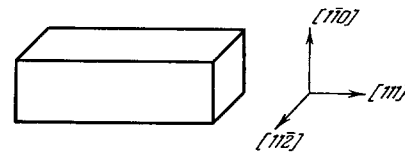


FIG. 21. Single crystal of NiO cut along the (111), (110) and (112) faces.

Therefore, a single-domain crystal suspended in a magnetic field tends to rotate so that the ferromagnetic layers in it are perpendicular to the magnetic field direction.

We shall consider a crystal of NiO cut along the faces (111), (110), and (112) and consisting entirely of a type I region (Fig. 21). Such a sample, suspended in a uniform magnetic field along the [110] axis, takes up an equilibrium position in which the direction [111] is parallel to the magnetic field H . If, by the application of an external stress along [112], the crystal is transformed completely into a type II region, the ferromagnetic layers become perpendicular to the [111] direction, which makes an angle of $70^{\circ}32'$ with [111] in the (110) plane. Consequently, in the new equilibrium position the crystal rotates about the [110] axis, by $70^{\circ}32'$ from the initial position. If this crystal consists of regions of two types I and II, then the new equilibrium position is given by an angle φ ($0 < \varphi < 70^{\circ}32'$)

$$\varphi = \frac{1}{2} \tan^{-1} \frac{4\sqrt{2}(1-q)}{16q-7},$$

where q is the ratio of the volume of a type I domain to the total volume of the crystal. Thus, by measuring the angle of rotation φ with respect to the magnetic field H , we can find the relationship between volumes of regions of type I and II in the crystal. The value of q may also be determined directly by the specular reflection method.

The motion of T-boundaries in various NiO samples was studied under the action of various external stresses. The measurements were carried out in a magnetic field of 2370 Oe. They showed that the force necessary to shift the T-boundaries was very small and in well-annealed samples it amounted to less than 10^6 dyne/cm². The mobility of the T-boundaries decreased considerably in the presence of various crystal defects and imperfections. It was found that a thin layer of cement deposited at the center of the surface of an annealed sample (Fig. 21) could fix the T-boundary positions. In unannealed poorly twinned crystals, in which the elastic energy density is high (10^5 erg/cm³), it was necessary to apply much greater stresses—of the order of 10^8 dyn/cm²—in order to set T-boundaries in motion.

During the motion of the T-boundaries through a crystal, an energy of 800 erg/cm³ per period was absorbed.^[17] One of the principal reasons for the absorption of energy was the irreversible spin rotation associated with the twinning of the crystal and the dis-

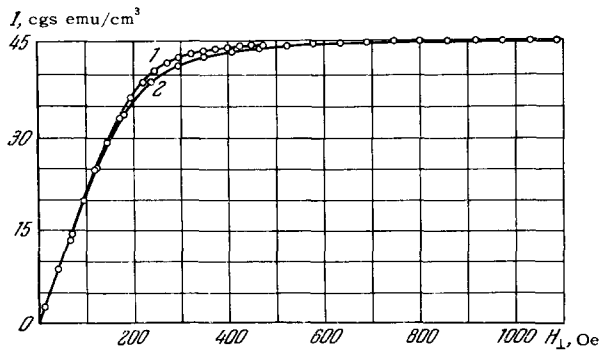


FIG. 22. Magnetization curves of CoCO_3 , measured at 4.2°K . 1) Measurements along a binary axis (direction of easy magnetization); 2) measurements along a direction perpendicular to the binary axis (hard magnetization axis).^[40]

placement of the T-boundaries.

The same method may be used to study the motion of T-boundaries under the action of a magnetic field. Measurements show that, in a well-annealed crystal, the T-boundaries move in fields from 5000 to 20 000 Oe.

A similar method can be applied successfully to study the T-domain structure of other antiferromagnets. The method of measuring the torque of an antiferromagnetic crystal suspended in a magnetic field can be used also to obtain some information on the distribution of S-domains in untwinned crystals. This method was used to study the magnetic anisotropy of single crystals of NiO, MnO, CoO,^[36,38] MnCO₃, and CoCO₃.^[39,40] The results of measurements indicate the presence of domains in these antiferromagnets.

We shall restrict ourselves to the case of CoCO₃. Kaczer^[40] investigated the magnetic anisotropy of this substance by measuring the torque of a crystal in a magnetic field using a magnetic torsion balance and a photocompensator. By this method, he determined the hexagonal anisotropy of CoCO₃ ($K_6 = 656 \pm 10 \text{ erg/cm}^3$) and its magnetization curve (Fig. 22). The ferromag-

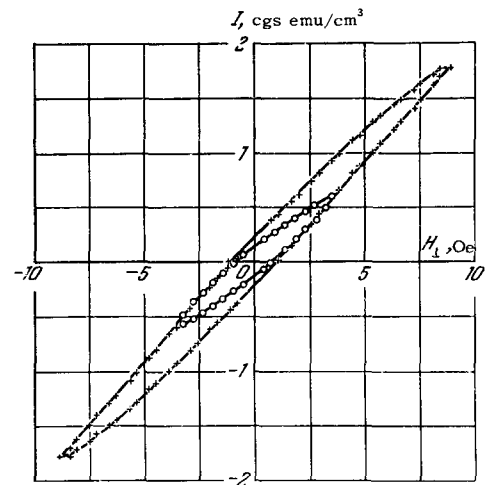


FIG. 23. Hysteresis loops, measured in weak fields along the easy magnetization direction ($T = 4.2^\circ\text{K}$).^[40]

netic moment at absolute saturation was $M_S = 45.3 \pm 1 \text{ G/cm}^3$ and the critical anisotropy field, 200–260 Oe. However, the magnetization saturation occurred in considerably stronger fields: 600–800 Oe. This meant that the domain structure of the crystal played an important part in its magnetization.

Figure 23 shows two hysteresis loops, recorded up to maximum fields of 3.5 and 9 Oe. The coercive forces H_C were 0.8 and 1 Oe, respectively, and the hysteresis losses were 1.3 and 5.3 erg/cm^3 . Calculations showed that the domain boundary displacement in CoCO₃ began in fields $H_k \approx 160 \text{ Oe}$, which were considerably stronger than those for hematite ($H_k \approx 10 \text{ Oe}$), but considerably weaker than those for the usual antiferromagnets ($H_k \approx 3000 \text{ Oe}$).

3.4. Investigation of Twinned Domain Structure by Means of X Rays

Two complementary methods were used to study the T-domain structure of the antiferromagnet NiO by means of x rays:^[24] the Berg-Barrett method and the x-ray back-reflection method. Photomicrographs were more convenient to obtain by the first method than the second. However, the first method did not show the T-domain structure if the angle of the relative tilt between the reflecting surfaces was very small. In that case, it was more convenient to use the back reflection method. Cleavage surfaces of unannealed NiO crystals were studied by these two methods.^[24] Photomicrographs of the T-domain structure of annealed and quenched crystals were also obtained. Saito^[24] obtained, in addition to his results which confirmed the studies of Roth and Slack, new important data on the T-domain structure of NiO, in particular on the interaction of the T-domain boundaries with crystal defects.

The T-domain structure, detected by x rays on cleavage surfaces of unannealed crystals, consisted of various laminar twins (Fig. 24).

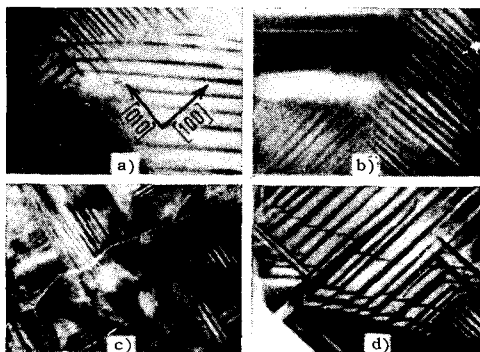


FIG. 24. Photomicrographs of cleavage surfaces of unannealed crystals. a) and b) Laminar twins meet one another at 90 and 45° ; c) complex domain structures with the majority of complex twins meeting at right angles; d) typical wedge-shaped domains; a four-face boundary structure is also visible.^[24]

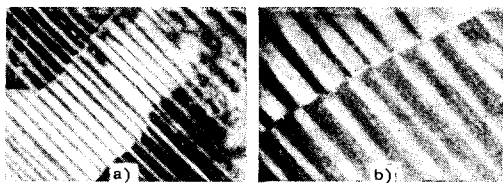


FIG. 25. T-boundaries intersecting grain boundaries.^[24]

Some departures of the T-boundaries from twin planes, characteristic of NiO, were detected. In complex structures, containing various laminar twins, many wedge-shaped domains were detected (Fig. 24). In a region where there was an accumulation of laminar domains, some departures from the lattice periodicity were possible, as well as a mismatch of crystallographic faces. Obviously, the formation of wedge-shaped domains in such regions was associated with a reduction in the elastic energy. In the majority of cases, the deviations of the T-boundaries from the usual crystallographic planes were small and could have been due to crystalline and magnetic imperfections.^[24]

Figure 25 shows the interaction of the T-boundaries with grain boundaries. In some cases, the T-boundaries penetrated the grain boundaries without interaction (Fig. 25a). In other cases the direction of the contraction axis changed on passing through the grain boundaries, without altering the domain shape and the relative positions of the domain boundaries (Fig. 25b). Sometimes, the grain boundaries were parallel to twin planes. In such cases, the grain boundaries could be distinguished from the T-boundaries in photomicrographs taken above the Néel temperature.

A large number of dislocations, produced by quenching, was observed on the surface of quenched samples. The surface density of the dislocations of such samples was 100 times greater than that for well-annealed samples, whose dislocation density (10^5 – 10^6 cm⁻²)

was estimated from the number of etch pits.^[25] It follows that dislocations may be one of the causes of the formation and stability of the T-domain structure in real crystals. It should be noted that in some cases the T-boundaries, which were of a certain size, did not interact with individual dislocations or groups of dislocations responsible for the short-range order stresses in the crystal. This was confirmed by the mobility of domain boundaries in annealed crystals.

Thus the interaction between T-boundaries and dislocations was obviously indirect. The T-domain structure was considerably affected by dislocations due to the elastic stresses produced by dislocations in the crystal.

3.5. Observations of Magnetic Domains in Antiferromagnets with Weak Ferromagnetism

The presence of a weak resultant magnetic moment in antiferromagnets with weak ferromagnetism makes it possible to observe domains by the methods usually employed to study domains in ferromagnets.

a) Magneto-optical method, based on the Faraday effect. This method was used to observe magnetic domains in hematite, α -Fe₂O₃, in transmitted polarized light.^[26]

The samples for the observation of domains were prepared in the form of films 2.5 μ thick whose surfaces were parallel to the (111) plane. Since the spins in α -Fe₂O₃ lay in that plane, the light was directed approximately at an angle of 45° to the film surface in order to observe the domains better. The domains with different directions of the magnetization vector rotated the plane of polarization of light to different extents, and therefore these domains were illuminated to different extents by the transmitted polarized light. The magnetic domains, visible as regions of different optical brightness, corresponding to different directions of magnetization, were observed only in the temperature range 250–950°K in which α -Fe₂O₃ had weak fer-

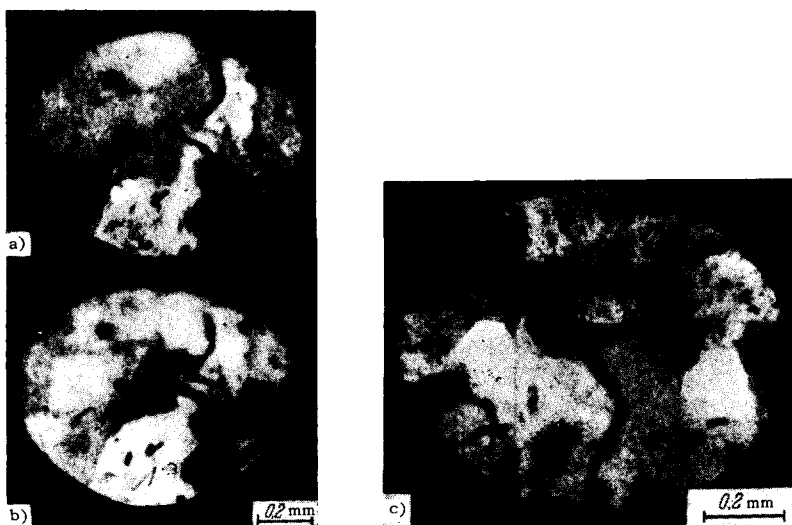


FIG. 26. Magnetic domains in (111) in a crystal of α -Fe₂O₃, observed by the Faraday effect. Comparison of a) and b) shows the change in the domain structure under the action of a magnetic field (10 Oe); c) domains of three different levels of brightness are visible.^[26]

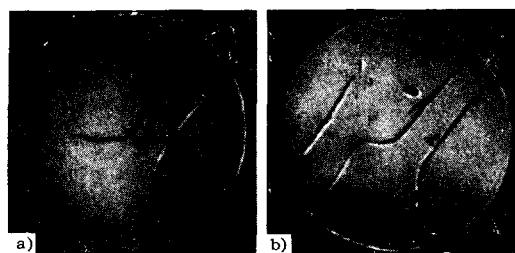


FIG. 27. Colloidal figures for a synthetic crystal of hematite: a) above the transition temperature, b) below the transition temperature.^[29]

romagnetism (Fig. 26). The domain structure of α - Fe_2O_3 changed on the application of a weak magnetic field (10 Oe) to a sample. The magnetostriction of α - Fe_2O_3 , due to its domain structure,^[7] accordingly appeared in weak fields.

The presence, in α - Fe_2O_3 , of domains having different directions of magnetization shows that weak ferromagnetism, in accordance with Dzyaloshinskii's theory,^[46] is an intrinsic property of this antiferromagnetic crystal and not the result of the magnetization of the domain boundaries.^[58]

The magneto-optical method was used also to study the domain structure of some orthoferrites of the MFeO_3 type, exhibiting weak ferromagnetism; here, M is yttrium or a rare-earth element.^[27] The results of these investigations are covered in the review of Williams and Sherwood.^[28]

This method, together with other magneto-optical methods, may be used to study the domain structure of other antiferromagnets with weak ferromagnetism.

b) Powder figure method^[29] was used to observe domains in larger synthetic crystals of hematite near the temperature of transition (-23°C) from the state with weak ferromagnetism (state II) to the purely antiferromagnetic state (state I).

The domain structure in hematite changed only slightly on cooling to temperatures short of the low-temperature transition. On reaching the critical temperature of -23°C , the powder figures broadened and disappeared (Fig. 27). If a sample was heated to a point slightly above the temperature of transition from state I to state II, the powder figures appeared again but not in the initial positions. Only after tens of such heat-treatment cycles, did the colloidal figures become similar, i.e., the hematite crystal exhibited a "memory effect" at the low-temperature transition. This effect was observed more clearly by the electron-shadow pattern method.^[30]

The powder figure method was used also to study domains in YFeO_3 .^[27]

c) Electron-shadow pattern method. Magnetic domains in natural hematite crystals were first investigated by Blackman, Haigh, and Lisgarten using this method.^[30] The method is based on the interaction of moving electrons with the leakage magnetic field of the

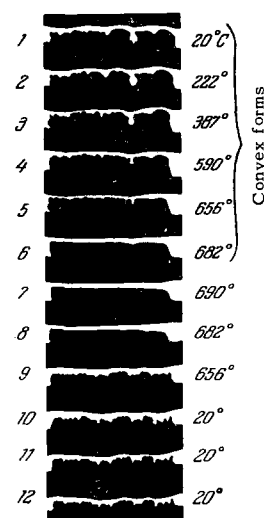


FIG. 28. Effect of temperature on electron shadow patterns for single crystals of hematite. The dimension of the crystal at right angles to the electron rays was 7mm.^[31]

sample's surface.

Kaye^[31] investigated the temperature dependence of the domain structure in hematite single crystals in the temperature range from 0° to 700°C in the terrestrial magnetic field. The majority of the crystals used had well-polished (001) faces. Some had polished (101), (223), and (014) faces.

Figure 28 shows some typical shadow patterns (1–8) for the surface of a crystal not subjected to a preliminary heat treatment. The crystal was then heated to 700°C and cooled in the terrestrial field. Interesting data were obtained on the temperature dependence of the shape and dimensions of the domains.

With gradual heating of the crystal, the positions of the convex forms in the powder patterns remained practically unchanged although their dimensions altered and some additional forms appeared. The dimensions of the convex forms remained practically constant up to 600°C ; in the temperature range from 600 to 680°C , their dimensions decreased rapidly and the forms disappeared completely at 680°C where the magnetic moment of the lattice vanished. All the convex forms varied with temperature in approximately the same way (Fig. 28, 1–6).

The dimensions of the convex forms, which were observed in various hematite crystals, were of the same order of magnitude and were independent of the type of surface (for example, (001), (104), etc.).

If a crystal was heated to a temperature lower than the Néel point (for example, to 10°C) and then cooled to room temperature, the powder patterns before and after heating were found to be the same (Fig. 29).

The heating of a crystal (not subjected to earlier heat treatment) to the Néel temperature and its subsequent cooling altered completely the initial shadow patterns (Fig. 28, 1 and 10). However, in crystals subjected to a preliminary heat treatment the shadow pat-



FIG. 29. Shadow patterns for hematite crystals: a) at room temperature; b) at 673°C; c) at room temperature after heating and cooling.^[31]

terns which appeared after repeated heat treatments were similar (Fig. 28, 10–12). Thus, for example, Fig. 28, 10–12, shows the results for a hematite crystal heated four times above the Néel temperature. Some change in details of the powder patterns was nevertheless detected after heat treatment. Thus hematite exhibited a partial “memory effect,” similar to the effect at the low-temperature transition.^[30]

The experimental results, obtained by the electron-shadow pattern method and by other methods, confirmed the domain structure of hematite associated with weak ferromagnetism. The average domain dimensions were 0.1 mm or more.

The slow variation of the shadow patterns on heating up to the Néel temperature shows that the domain structure of hematite is very stable in the temperature range 250–970°C.

These data, together with the theoretical calculations,^[49] allow us to draw the conclusion that the domain structure in weakly ferromagnetic antiferromagnets of the $\alpha\text{-Fe}_2\text{O}_3$ type is due to the existence of demagnetizing fields.

4. CONDITION FOR THE EXISTENCE OF THE DOMAIN STRUCTURE IN ANTIFERROMAGNETS AND ITS STABILITY

The domain structure in antiferromagnets exhibiting weak ferromagnetism may be due to demagnetizing fields, if the anisotropy constant, which plays the main role in the formation of domain boundaries, is small. Among such antiferromagnets are $\alpha\text{-Fe}_2\text{O}_3$, MnCO_3 , CoCO_3 , NiF_2 , etc., in which magnetic domains have been discovered by various methods. For example, the magnetic anisotropy of hematite is very low in the (111) plane containing the spins. The effective sixth-order anisotropy constant, which plays the main role in the formation of domain boundaries in hematite, has a value of only 3 erg/cm³,^[53] i.e., 10^6 – 10^8 times smaller than the second-order anisotropy constant. Therefore, in antiferromagnets having weak ferromagnetism, the domain-boundary energy density is very low (0.01 erg/cm² for hematite).^[49] The presence of a weak resultant magnetic moment ($m \sim v^2/c^2 \sim 10^{-4}$) is sufficient for the formation of the domain structure

Table II

Antiferromagnets	Effective anisotropy constant, erg/cm ³	Δw , erg/cm ²	D, mm	δ , mm
$\alpha\text{-Fe}_2\text{O}_3$	3	$2 \cdot 10^{-2}$	1	10^{-2}
MnCO_3	1	$1 \cdot 10^{-3}$	1	10^{-2}
CoCO_3	660	$2 \cdot 10^{-2}$	0.1	10^{-4}

in such antiferromagnets due to demagnetizing fields.^[49] According to calculations, the domain dimensions for $\alpha\text{-Fe}_2\text{O}_3$ are larger than those for ferromagnets, reaching 1 mm, in agreement with the experimental results (Sec. 3).

Table II lists the transition-layer thickness (δ), and the optimum domain dimensions (D) for weak ferromagnets of the $\alpha\text{-Fe}_2\text{O}_3$ type.^[49]

Antiferromagnets free from weak ferromagnetism do not exhibit resultant magnetization in the absence of an external magnetic field. Nevertheless, there are several mechanisms responsible for the appearance and stability of the domain structure in such antiferromagnets.

The possibility of the formation of the “domain structure” in ordered structures (in particular, the domain structure in antiferromagnets) and their stability have been discussed, on kinetic grounds, in a recent work by I. M. Lifshitz.^[54]

In the usual isotropic ordered alloys, the formation of structural domains is impossible if there are only two equivalent structures (the long-range parameter $\pm \eta$). In this case the ordering of the crystal at phase transitions of the second kind occurs not by uniform relaxation or by a seed mechanism, but by a process characteristic of the formation of web-like ordered regions and their subsequent growth, in which the “driving force” is the surface energy at the boundary between elementary regions (Fig. 30). However, in the isotropic case and in the absence of a correlation between neighboring elementary regions, such a growth does not lead finally to the domain structure formation: a single ordered region should form throughout the crystal.^[54]

However, when a sample contains several thermodynamically equivalent structures (η_k , $k = 1, 2, \dots, p$, where $p \geq 4$), the initial relaxation stage does not give

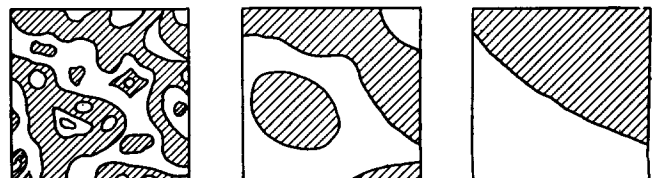


FIG. 30. Ordering of isotropic structures in the presence of two thermodynamically equivalent regions.^[54]

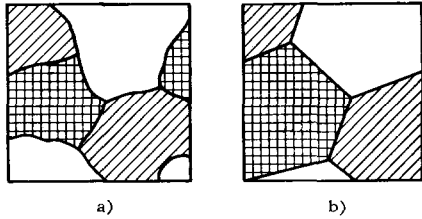


FIG. 31. Formation of domains on ordering in the case of several thermodynamically equivalent structures.^[54]

rise to the formation of interlocking web-like regions, as in the case of two equivalent structures ($\pm\eta$), but each small elementary region (a domain), having structure η_k , is very likely to be surrounded by elementary regions of different types (Fig. 31a). Points where three or four elementary regions meet are lines and points of intersection of several domain boundaries.

The presence of these points and lines considerably affects the further development of the elementary regions. By virtue of the dynamic equivalence of each of the structures (η_k), further relaxation reduces to the motion of the domain boundaries, which lowers their energy. This leads to a gradual straightening of the elementary region boundaries (Fig. 31b). However, the condition for a surface energy minimum requires the formation of optimum angles near the contact lines and points. When the optimum angles are established at all contact lines and points throughout a crystal, the displacement of a boundary becomes very difficult and, in fact, any movement of a contact point becomes impossible.

Thus, ordered structures may have a "domain structure" which is not energetically favored but is stable from the kinetic point of view. Such a domain structure may be destroyed only by external agencies (deformation, magnetic field) which make some of the structures η_k thermodynamically preferred.^[54]

These conditions are satisfied, above all, by the formation of the T-domain structure in antiferromagnets of the NiO, MnO, etc., type, in which four different types of domain may be formed. Experiments indicate (Sec. 3.2b) that the most stable combination in annealed crystals is that which consists of four domains.

The results described above were obtained on the assumption that the rate of growth of individual ordered regions is isotropic. However, as was first pointed out by Néel,^[41] the formation of domains in antiferromagnets is affected considerably by the anisotropy and magnetoelastic forces, which tend to restrict the sublattice magnetization vectors to certain crystallographic directions and prevent the motion of domain boundaries. I. M. Lifshitz^[54] showed that the situation is affected markedly even by the anisotropy of the rate of change of domains, which is associated with the difference between exchange interactions along various crystallographic directions and with the anisotropy forces in antiferromagnets. In this case, the do-

main structure is possible also in uniaxial antiferromagnets with two different domains. This applies both to the twinned domain structure and to the S-domain structure. The domain structure (T- or S-type), stable according to kinetic considerations, is in the metastable state and represents a relative free-energy minimum and not the absolute minimum.

The conditions for the formation of T-boundaries and their orientation in NiO were investigated by Ymada.^[55] He determined the law of spin rotation in a transition layer, calculated the layer thickness (40 Å) and the energy density in T-boundaries (3.5 erg/cm²).

A twinned domain structure is formed when there is antiferromagnetic ordering in a crystal. Below the Néel temperature, antiferromagnetic crystals are deformed by contraction (or expansion) of the crystal lattice along certain crystallographic directions and, as a result of this stressed state, the twinned domain structure, which reduces the magnetoelastic energy, may be formed in some antiferromagnets (NiO, MnO). The T-domain structure stability in the antiferromagnets NiO and MnO is accounted for by the kinetic considerations. In well-annealed crystals, the T-boundaries move easily. The T-boundary mobility may be restricted by crystal defects and impurities. In real crystals, the T-domain structure depends on the long-range internal stresses caused by the presence of various crystal defects.

The presence of points of contact of T-domain boundaries in antiferromagnets fixes certain domain boundary positions but does not exclude the possibility of motion about equilibrium positions due to thermal excitation. The mobility of domain boundaries is greater in the absence of points or lines of contact between several domain boundaries.

In contrast to T-boundaries, the energy minimum for S-domain boundaries in antiferromagnets corresponds, in general,^[56-58] to several S-boundary positions or several combinations of the spin orientation in the transition layer. Consequently, in some antiferromagnets the formation of S-domain boundaries may be found to be thermodynamically preferred from entropy considerations.

The S-domain boundary formation in antiferromagnets below the Néel temperature is associated with a departure from the long-range order and leads, on the one hand, to an increase in the energy of the transition layer, and on the other, to an entropy increase. The latter is associated with the fact that the domain boundary positions in antiferromagnets are not rigorously fixed because of the absence of demagnetizing fields. As a result of thermal motion, the domain boundaries may shift from the equilibrium positions by distances of several lattice periods.^[58] Moreover, because of thermal motion, there are many ways of spin rotation in a transition layer. The energy increase reduces the free energy of the transition layer.

Li^[58] showed that in antiferromagnets the energy

Table III

Antiferromagnets	NiO	MnO	Cr ₂ O ₃	MnF ₂	FeF ₂	CuCl ₂ ·2H ₂ O
Δw , erg/cm ³	0.15	0.5	4.6	7.3	17	0.14
Transition layer thickness	3·10 ⁻⁵	6·16 ⁻⁶	3·10 ⁻⁶	1·10 ⁻⁶	8·10 ⁻⁸	3·10 ⁻⁶

increase in the transition layer may be compensated by the entropy increase. The formation of domain boundaries in antiferromagnets is thermodynamically preferred if the free-energy increase is negative:

$$\Delta F = \Delta w - T\Delta S < 0. \quad (4.1)$$

Here, Δw is the energy increase in the transition layer and ΔS is the entropy increase.

The energy increase in the transition layer may be calculated from the condition for a domain-boundary energy minimum. The order of magnitude of the energy density in the domain boundaries is given by the formula

$$\Delta w \sim a_0 \sqrt{H_e K_e M_0}, \quad (4.2)$$

where H_e is the effective exchange interaction field,

$$H_e \sim \frac{M_0}{\chi_{\perp}}, \quad (4.3)$$

χ_{\perp} is the transverse susceptibility, K_e is the effective anisotropy constant, a_0 is the lattice constant. Using a formula similar to Eq. (4.2), the energy densities in domain boundaries have been calculated for some antiferromagnets. According to the calculations of Moriya,^[59] the energy density is 0.2 erg/cm² for 180° domain boundaries, parallel to the (a, b) plane, in NiF₂. Antiferromagnets with weak ferromagnetism (cf. Table II) and antiferromagnets of the NiO type (Table III) have low energy density in the domain boundaries. For uniaxial antiferromagnets (Cr₂O₃, MnF₂, etc.), the energy density in the domain boundaries is considerably greater (cf. Table III).

Li^[58] showed that the contribution of the entropy of domain boundaries, due to their mobility, can be given approximately by the formula

$$\Delta S \approx \frac{A}{n^2} \ln p, \quad (4.4)$$

where Aa_0^2 is the domain boundary area, n is the average value of its displacement in units of a_0 , and p is the number of various ways of measuring the domain boundary position. The formula (4.3) is obtained on the assumption that the displacements of domain boundaries do not greatly increase their energy. Then, using Eqs. (4.2) and (4.3), the condition (4.1) may be represented as

$$\Delta F \approx a_0 (H_e K_e M_0)^{\frac{1}{2}} - \frac{1}{n^2 a_0^2} \kappa T \ln p < 0, \quad (4.5)$$

where κ is Boltzmann's constant. However, in the formula (4.3), the method of calculating p is an open question, and this formula may serve only to obtain estimates of the free-energy increase in the transition layer.^[58] To obtain more accurate estimates of whether the domain boundary formation in antiferromagnets is thermodynamically favored, it is necessary to use more rigorous methods of calculating the free-energy increase in the transition layer.

The method of calculating the free-energy and entropy increases in the transition layers of the structural domains in ordered structures (alloys) has been given by Cahn and Kikuchi^[56] for the temperature of absolute zero, and by Kikuchi and Cahn^[57] for non-zero temperatures.

The free energy increase in the transition layer has been calculated by the present author^[48] by a method based on the determination of the spectrum of elementary excitations.

In an antiferromagnetic sample with a domain structure, there are several types of elementary excitation.^[48] Some of them are characteristic of the domains and of the transition layer, and others of the transition layer only.

The activation energy of the elementary excitations that are characteristic only of the transition layer is the lowest and, therefore, it is important in the study of nuclear magnetic resonance in antiferromagnets.^[60]

To calculate the free-energy increase in the transition layer it is necessary to use those elementary excitation modes which are characteristic only of the transition layers. The elementary excitations characteristic both of the domains and of the transition layer do not greatly affect the free-energy increase in the transition layer.

We shall denote the energy spectrum of the elementary excitations that are characteristic only of the transition layer by

$$\varepsilon_{hi} = \varepsilon_{hi}(\mathbf{k}), \quad (4.6)$$

where $i = 1, 2, \dots$ is the number of energy spectrum modes, \mathbf{k} is the wave vector. The energy gap for each mode is denoted by ε_{0i} . The actual forms of the dispersion law (4.6) and the values of the energy gap for different antiferromagnets are given in^[48]. In the case of a transition layer in NiO, there is one energy spectrum mode, while for the antiferromagnets Cr₂O₃

Table IV

Antiferromagnets	NiO	MnO	Cr ₂ O ₃	MnF ₂	CuCl ₂ ·2H ₂ O
$T_D, ^\circ\text{K}$	100	63	260	64	—
$T_N, ^\circ\text{K}$	523	118	307	67	4.3

and CuCl₂·2H₂O there are two modes. When the finite domain dimensions and their coupling are allowed for, each of these modes splits further into two modes with similar energy gaps.

The increase in the free-energy density,^[48] calculated per unit area of the domain boundary, may be represented as

$$\Delta F = \Delta w - \frac{\delta\chi_{\perp}^{3/2}}{6\pi^2\gamma^3h} J_1 \sum_i J_{2i}. \quad (4.7)$$

Here, the value of the integral J_1 depends on the crystal symmetry.^[48] The order of magnitude is

$$J_1 \sim \chi_{\perp}^{3/2} a_0^{-3/2} (2M_0)^{-3}.$$

The value of the integral J_{2i} may be calculated in its general form. We shall consider here only two simple special cases which are of great practical importance.

First case:

$$\frac{\epsilon_{0i}}{\kappa} \ll T < T_N, \\ J_{2i} = (\kappa T)^4 \left(\frac{\pi^2}{15} - \frac{\pi^4}{4} \xi_{0i}^2 \right); \quad (4.8)$$

Second case:

$$T \ll \frac{\epsilon_{0i}}{\kappa}, \\ J_{2i} = 3 \sqrt{\frac{\pi}{2}} (\kappa T)^4 \xi_{0i}^{-3/2} \left(1 - \frac{21}{8\xi_{0i}^2} \right) e^{-\xi_{0i}}, \quad (4.9)$$

where

$$\xi_{0i} = \frac{\epsilon_{0i}}{\kappa T}.$$

It follows from Eq. (4.7) that the entropy increase in the transition layer is associated with the appearance of additional types of elementary excitation, characteristic only of the transition layer.

Using the formulas (4.7)–(4.9) for various antiferromagnets, we may check whether the following inequality is satisfied

$$\Delta F < 0. \quad (4.10)$$

It follows from Eqs. (4.10) and (4.8) that for each antiferromagnet there is a temperature interval $T_D < T < T_N$, in which the inequality (4.10) is satisfied. In that interval, the entropy term of the free energy exceeds the energy increase in the transition layer, and the formation of domain boundaries and antiferromagnets is thermodynamically favored.

It follows from Eq. (4.8) that if the energy gap is small ($\xi_{0i} \ll 1$), the contribution of the entropy to the

free energy is proportional to the fourth power of the absolute temperature.

Table IV lists the values of the temperature T_D for various antiferromagnets.

It is evident from this table that in antiferromagnets of the NiO type with many antiferromagnetic axes the formation of domain boundaries is thermodynamically favored over quite a wide range of temperatures ($T_D < T < T_N$). In antiferromagnets with a single antiferromagnetic axis (MnF₂, Cr₂O₃), this range is considerably narrower and lies near the Néel temperature. The inequality (4.10) is not satisfied at all by some antiferromagnets (for example, CuCl₂·2H₂O, FeF₂).

In antiferromagnets with weak ferromagnetism (α -Fe₂O₃, MnCO₃, CoCO₃) the entropy contribution may be important, along with the demagnetization factor, in the formation of the domain structure.

In calculating the value of T_D (cf. Table IV), the possible defects in crystals were not allowed for. Therefore, the calculated values of T_D refer to "pure" crystals whose properties are approximated by annealed crystals. For real crystals, the value of T_D depends on the treatment of the sample.

Below the temperature T_D ($T < T_D$), the formation of domain boundaries is not favored by thermodynamic considerations. The entropy term reduces the free energy but it cannot compensate it completely.

The domain structure in antiferromagnets may also exist below the temperature T_D ($T < T_D$). Such a domain structure may be formed in the process of magnetic ordering. Domains may also be formed when twinning takes place in a crystal (cf. Secs. 2–3). The position of S-boundaries in real antiferromagnets may be governed by various crystalline and magnetic defects.^[16–19]

¹ "Itogi nauki" (Progress in Science), No. 4, Antiferromagnetizm i ferrity (Antiferromagnetism and Ferrites), AN SSSR, 1962; Nagamia, Yosida, and Kubo, Advances in Physics 4(13), 1 (1955).

² L. Néel, Ann. phys. 3, 137 (1948) (cf., Russ. transl. in collection "Antiferromagnetizm" (Antiferromagnetism), M., IL, (1956); L. Néel, Proc. Intern. Conference Theor. Phys. (Kyoto and Tokyo, Sept. 1953), Tokyo, 1954.

³ K. P. Belov and R. Z. Levitin, JETP 37, 565 (1959), Soviet Phys. JETP 10, 400 (1960).

⁴ T. Nakamichi and M. Yamamoto, J. Phys. Soc. Japan 16, 126 (1961).

⁵ L. Alberts and E. W. Lee, Proc. Phys. Soc. (London) 78, 728 (1961).

⁶ T. R. Guire and W. A. Crapo, J. Appl. Phys., Suppl. 33, 1291 (1962).

⁷ H. M. A. Urquart and J. E. Goldman, Phys. Rev. 101, 1443 (1956).

⁸ Belov, Kataev, and Levitin, JETP 37, 938 (1959), Soviet Phys. JETP 10, 670 (1960).

- ⁹ A. A. Evtushenko and R. Z. Levitin, *FMM* **12**, 155 (1961).
- ¹⁰ K. P. Belov and R. Z. Levitin, in collection: "Ferrity" (Ferrites), Minsk, AN BSSR, 1960.
- ¹¹ R. Z. Levitin, Dissertation (Ural State University, 1962).
- ¹² R. Street and B. Lewis, *Nature (London)* **168**, 1036 (1951); *Proc. Phys. Soc. (London)* **72**, 604 (1958); *Phil. Mag.* **1**, 663 (1956).
- ¹³ M. E. Feine, *Phys. Rev.* **87**, 1143 (1952).
- ¹⁴ Makkay, Geiger, and Fine, *J. Appl. Phys.* **33**, 914 (1962).
- ¹⁵ R. Street and J. H. Smith, *J. phys. radium* **20**, 82 (1959).
- ¹⁶ W. L. Roth and G. A. Slack, *J. Appl. Phys., Suppl.* **31**, 352 (1960).
- ¹⁷ G. A. Slack, *J. Appl. Phys.* **31**, 1571 (1960).
- ¹⁸ W. L. Roth, *Phys. Rev.* **111**, 772 (1958).
- ¹⁹ W. L. Roth, *J. Appl. Phys.* **31**, 2000 (1960).
- ²⁰ Wilkinson, Cable, Wollan, and Koehler, *Phys. Rev.* **113**, 497 (1959).
- ²¹ Koehler, Wilkinson, Cable, and Wollan, *J. phys. radium* **20**, 180 (1959).
- ²² Alperin, Brown, Nathans, and Picart, *Phys. Rev. Letters* **8**(6), 237 (1962); G. Shirane, Symposium on Ferromagnetism and Ferroelectricity, May 30—June 5, 1963, Leningrad; Picart, Nathans, and Alperin, *J. Appl. Phys.* **34**, 1200 (1963).
- ²³ H. H. Kondoh, *J. Soc. Japan* **17**, 1316 (1962); *J. Phys. Soc. Japan* **18**, 595 (1963).
- ²⁴ S. Saito, *J. Phys. Soc. Japan* **17**, 1287 (1962).
- ²⁵ T. Takeda and H. Kondoh, *Phys. Soc. Japan* **17**, 1317 (1962).
- ²⁶ Williams, Sherwood, and Remeika, *J. Appl. Phys.* **29**, 1772 (1958).
- ²⁷ Sherwood, Remeika, and Williams, *J. Appl. Phys.* **30**, 217 (1959).
- ²⁸ *Magnitnye svoïstva metallov i splavov (Magnetic Properties of Metals and Alloys)*, M., IL, 1951.
- ²⁹ M. Blackman and B. Gustard, *Nature* **193**, No. 4813, 360 (1962).
- ³⁰ Blackman, Haigh, and Listgarten, *Nature* **179**, 1288 (1957); *Proc. Roy. Soc. (London)* **A251**, 117 (1959).
- ³¹ G. Kaye, *Proc. Phys. Soc. (London)* **78**, 869 (1961).
- ³² R. G. Shulman, *J. Appl. Phys., Suppl.* **32**, 126 (1961).
- ³³ Matsuura, Yasuoka, Hirai, and Hashi, *J. Phys. Soc. Japan* **17**, 1147 (1962); Le Dang Khoi and F. Bertaut, *Compt. rend.* **254**, 1584 (1962).
- ³⁴ H. Kondoh, *J. Phys. Soc. Japan* **15**, 1970 (1960).
- ³⁵ G. T. Rado and V. J. Folen, *Phys. Rev. Letters* **20**, 310 (1960); *J. Phys. Soc. Japan* **17**, Suppl. B-1, 244 (1962); D. N. Astrov, *JETP* **40**, 1333 (1961), *Soviet Phys. JETP* **13**, 938 (1961).
- ³⁶ Kondoh, Uchida, Nakazumi, and Nagamia, *J. Phys. Soc. Japan* **13**, 579 (1958); Kondoh, Uchida, and Nakazumi, *J. Phys. Soc. Japan* **17**, 1318 (1962).
- ³⁷ Uchida, Kondoh, Nakazumi, and Nagamia, *J. Phys. Soc. Japan* **15**, 466 (1960).
- ³⁸ J. R. Singer, *Phys. Rev.* **104**, 929 (1956).
- ³⁹ A. S. Borovik-Romanov, *JETP* **36**, 766 (1959), *Soviet Phys. JETP* **9**, 539 (1959).
- ⁴⁰ Ya. Katser, *JETP* **43**, 2042 (1962), *Soviet Phys. JETP* **16**, 1443 (1963).
- ⁴¹ L. Néel, *Izv. AN SSSR, ser. fiz.* **21**, 890 (1957), *Columbia Tech. Transl.* **21**, 889 (1957); W. J. Haas and B. H. Schultz, *J. phys. radium* **10**, 7 (1939).
- ⁴² C. J. Gorter, *J. phys. radium* **12**, 275 (1951) (cf. Russ. transl. in collection "Antiferromagnetizm" (Antiferromagnetism), M., IL, 1956).
- ⁴³ A. Arrot and B. R. Coles, *J. Appl. Phys., Suppl.* **32**, 51 (1961).
- ⁴⁴ Collection: "Antiferromagnetizm" (Antiferromagnetism), M., IL, 1956; S. V. Vonsovskii and Yu. M. Seidov, *DAN SSSR* **107**, 37 (1956), *Doklady* **1**, 149 (1956).
- ⁴⁵ A. W. Overhauser, *Phys. Rev.* **128**, 1437 (1962); C. Herring, *Revs. Modern Phys.* **34**, 631 (1962).
- ⁴⁶ I. E. Dzyaloshinskiĭ, *JETP* **32**, 1547 (1957), *Soviet Phys. JETP* **5**, 1259 (1957).
- ⁴⁷ E. A. Turov, *Fizicheskie svoïstva magnitouporyadchennykh kristallov (Physical Properties of Magnetically Ordered Crystals)* M., AN SSSR, 1963; English translation published by Academic Press 1965.
- ⁴⁸ M. M. Farztdinov, *FMM* (in press).
- ⁴⁹ M. M. Farztdinov, Symposium on Ferromagnetism and Ferroelectricity, May 30—June 5, 1963, Leningrad.
- ⁵⁰ J. I. Kaplan, *J. Chem. Phys.* **22**, 1709 (1954).
- ⁵¹ A. L. Loeb and J. B. Goodenough, Conference on Magnetism and Magnetic Materials, Boston, Massachusetts, October 16—18, 1958.
- ⁵² C. Kittel, *UFN* **41**, 452 (1950).
- ⁵³ Kumagai, Abe, Ono, Haysashi, Shimada, and Iwanada, *Phys. Rev.* **99**, 1116 (1955); E. A. Turov and N. G. Guseĭnov, *JETP* **38**, 1326 (1960), *Soviet Phys. JETP* **11**, 955 (1960).
- ⁵⁴ I. M. Lifshitz, *JETP* **42**, 1354 (1962), *Soviet Phys. JETP* **15**, 939 (1962).
- ⁵⁵ T. Ymada, *J. Phys. Soc. Japan* **18**(4), 520 (1963).
- ⁵⁶ J. W. Cahn and R. Kikuchi, *J. Phys. Chem. Solids* **20**, 94 (1961).
- ⁵⁷ R. Kikuchi and J. Cahn, *J. Phys. Chem. Solids* **23**, 137 (1962).
- ⁵⁸ Y. Y. Li, *Phys. Rev.* **101**, 1450 (1956).
- ⁵⁹ T. Moriya, *Phys. Rev.* **117**, 635 (1960).
- ⁶⁰ D. I. Paul, *Phys. Rev.* **126**, 78 (1962); *Phys. Rev.* **127**, 455 (1962); *Phys. Rev.* **131**, 178 (1963).

Translated by A. Tybulewicz